

**ENDOVENOUS LASER ABLATION: DIFFERENT LASERS
AND DELIVERY TECHNIQUES**

by

MERAL FİLİZ SOMUNYUDAN

BS., in Physics Engineering, Istanbul Technical University, 2007

Submitted to the Institute of Biomedical Engineering
in partial fulfillment of the requirements
for the degree of
Master of Science
in
Biomedical Engineering

Boğaziçi University

2011

**ENDOVENOUS LASER ABLATION: DIFFERENT LASERS
AND DELIVERY TECHNIQUES**

APPROVED BY:

Assoc. Prof. Dr. Murat GÜLSOY

(Thesis Advisor)

Assoc. Prof. Dr. Ata AKIN

Assist. Prof. Dr. Mehmet Ümit ERGENOĞLU

DATE OF APPROVAL: 13 June 2011

ACKNOWLEDGMENTS

First and foremost, I offer my sincerest gratitude to my supervisor, Assoc. Prof. Murat Gülsoy who has supported me throughout my thesis with his patience and knowledge. I attribute the level of my Masters degree not to only his encouraging guidance every time, but also his ability about looking at each event from different point of view that contributes me for exceeding difficulties during each moment of this study. This thesis would not be possible without his kind support and the remarkable patience.

I owe my appreciate to members of my committee, Assist. Prof. Dr. Mehmet Ümit Ergenoğlu for being a my thesis progress committee and his valuable contributions and suggestions and Assoc. Prof Ata Akın for allocating his time for critical reviewing of this thesis. It is a pleasure to thank to Dr. Ferda Özkan for providing technical support during histological procedure of this thesis.

This work would not be possible without the help of my colleagues and friends Özgür Tabakoğlu, Nermin Topaloğlu, Ayşe Sena Kabaş Sarp, Burcu Tunç, Gamze Bölükbaşı, Özgür Kaya and Çağlar Gök. I owe my deepest gratitude to Emrah Aytolu for providing moral, technical support, knowledge and motivation during my thesis. I am deeply grateful to Evren Coşkun Özüer who always stood by me with the different point of view, his love, emotional support and patience.

Finally, this thesis is dedicated to my parents, my mother Nebahat Somunyudan and my father Mahmut Somunyudan who have given me the opportunity of an education from the best institutions, support throughout my life and whose constant encouragement and never-ending love I have relied throughout my life.

ABSTRACT

ENDOVENOUS LASER ABLATION: DIFFERENT LASERS AND DELIVERY TECHNIQUES

Endovenous Laser Ablation (EVLA) has become a popular minimally invasive alternative to stripping in the treatment of saphenous vein reflux. Several wavelengths have been proposed; of which 810, 940 and 980- nm are the most commonly used. Thermal shrinkage of collagenous tissue during EVLA plays a significant role in the early and late results of the treatment. Longer wavelengths (>1000 -nm) show greater water absorption than shorter wavelengths and may have some advantages for EVLA due to water molecules in the vein lumen cells. However, the most appropriate wavelength is still the subject of debate. The laser light delivery technique is another criteria that affect the success of EVLA. Bare fiber, which is generally used for medical application, delivers the laser light locally focused to application area. Radial fiber, which is a new technique for laser light delivery, emanates the laser energy homogenously circularly to vessel lumen.

The aim of this study is to compare the efficacy of 980 and 1940-nm laser wavelengths in the treatment of varicose veins. In this study, 980 and 1940-nm lasers were used to irradiate stripped human veins. Different power settings (8/10W for 980-nm, 2/3W for 1940-nm) and laser delivery techniques (radial and bare fiber) were used to compare their effects. As a conclusion, 1940-nm TM-fiber laser and radial fiber are promising methods in the treatment of varicose veins.

Keywords:Endovenous Laser Ablation, 1940-nm, 980-nm, Radial Fiber, Bare Fiber, Varicose Vein

ÖZET

ENDOVENÖZ LASER UYGULAMASI: FARKLI LASERLER VE FARKLI IŞIK YAYIM TEKNİKLERİ

Varis tedavilerinde Endovenöz Laser Uygulaması (EVLA), son yıllarda klasik cerrahi yöntem olan Vena Safena Magna Strippinge göre daha güvenli, verimli ve çok az girişimsel olduğu için daha popüler hale gelmiştir. EVLA'nın başlıca uygulama prensibi damar lümeninin kolojen dokusunun, laser ışığı ile termal hasara uğratarak daraltılmasıdır. EVLA yeni bir yöntem olduğu için uygulanan optimum dalgaboyu, güç ve kullanılan fiber gibi uygun parametreler üzerinde hala çalışılmaktadır. EVLA için çeşitli dalga boyları kullanılmaktadır; bunlardan 810, 940 ve 980-nm en çok kullanılan dalga boylarıdır. 1000-nm den daha büyük olan dalga boyları, su tarafından daha iyi bir emilim gösterdiği için, laser ışığının damar dokusunda bulunan su molekülleri tarafından kuvvetli bir emilime uğrayabileceği düşünüldüğünde daha iyi sonuçlar verebilir. Laser ışığının fiber ucundan yayılım şekli de EVLA sonucunu etkileyebilecek parametreler arasındadır. Klinik çalışmalarda genelde düz uçlu fiber kullanılır. Bu fiberde ışık tek bir noktadan çıkarak damar içinde dağılır. Radyal fiber ise klinik çalışmalarda yeni kullanılmaya başlayan ve iyi sonuçlar veren bir fiberdir. Bu fiberde ışık yayılımı radyal fiber ucu etrafında 360° olarak homojen yayılır.

Bu çalışmada optimum güç, dalga boyu ve fiberi bulabilmek için insanlardan klasik cerrahi yöntem ile çıkarılan damarların iç yüzeyine klinik çalışmalarda en çok kullanılan 980-nm diyot laser ile, su tarafından emilimi çok yüksek olan 1940-nm laser hem bare hem de radial fiber kullanılarak uygulanmıştır. 980-nm diyot laser için 8W ve 10W güç kullanılırken, 1940-nm Tm fiber Laser için 2W ve 3W seçilmiştir. Sonuç olarak, 1940-nm Tm Laser ve radyal fiber EVLA için umut verici bir yöntemdir.

Anahtar Sözcükler: Endovenöz Laser Uygulaması, EVLA, 1940-nm Tm Fiber Laser, 980-nm Diyot Laser, Varis, Radyal Fiber, Düz Uçlu Fiber.

TABLE OF CONTENTS

ACKNOWLEDGMENTS	iii
ABSTRACT	iv
ÖZET	v
LIST OF FIGURES	viii
LIST OF TABLES	xiii
LIST OF ABBREVIATIONS	xiv
1. INTRODUCTION	1
1.1 Motivation and Objectives	1
1.2 Outline	2
2. BACKGROUND	4
2.1 Varicose Veins	4
2.1.1 Structure of the Vein Wall	4
2.1.1.1 Great Saphenous Vein (GSV)	6
2.1.1.2 Small Saphenous Vein (SSV)	6
2.1.2 Structure of Varicose Vein	7
2.1.3 Treatment Techniques	9
2.1.3.1 Surgical Ligation and Stripping (Phlebectomy)	9
2.1.3.2 Radiofrequency ablation (RFA)	10
2.1.3.3 Endovenous Chemical Ablation	11
2.1.3.4 Endovenous Laser Ablation	11
3. METHODS	18
3.1 Human Veins	18
3.2 Lasers and Fibers	18
3.3 Laser Application Procedure	22
3.4 Histological Procedure	24
3.4.1 Tissue Processing	24
3.4.2 Paraffin Embedding	26
3.4.3 Tissue Sectioning	26
3.4.4 Tissue Staining	27

4. RESULTS	30
4.1 Laser Application Results	30
4.1.1 980-nm Diode Laser Application with Bare Fiber and Radial Fiber	31
4.1.1.1 Decrease in Inner and Outer Diameter	31
4.1.1.2 Operation Time	31
4.1.1.3 Energy per Length	32
4.1.1.4 The Amount of Energy Delivered for 1 mm Shrinkage .	33
4.1.2 1940-nm Fiber Laser Application with Bare Fiber and Radial Fiber	34
4.1.2.1 Decrease in Inner and Outer Diameter	34
4.1.2.2 Operation Time	36
4.1.2.3 Energy per Length	36
4.1.2.4 The Amount of Energy Delivered for 1 mm Shrinkage .	37
4.1.3 Comparison of 980-nm Diode Laser and 1940-nm Fiber Laser	
Application with Bare Fiber	37
4.1.3.1 Decrease in Inner and Outer Diameter	37
4.1.3.2 Operation Time	38
4.1.3.3 Energy per Length	39
4.1.3.4 The Amount of Energy Delivered for 1 mm Shrinkage .	39
4.1.4 Comparison of 980-nm Diode Laser and 1940-nm Fiber Laser	
Application with Radial Fiber	41
4.1.4.1 Decrease in Inner and Outer Diameter	41
4.1.4.2 Operation Time	41
4.1.4.3 Energy per Length	42
4.1.4.4 The Amount of Energy Delivered for 1 mm Shrinkage .	43
4.2 Histological Procedure Results	44
5. DISCUSSION	49
6. CONCLUSION	54
REFERENCES	55

LIST OF FIGURES

Figure 2.1	The veins consists of three layer: Tunica Adventita, Tunica Media and Tunica Intima. Tunica Intima has valves to keep blood flow in one direction [1].	5
Figure 2.2	The veins consists of three layer: Function of the valves in the veins [2].	6
Figure 2.3	A: The pathway of the Great Saphenous Vein (GSV); B: The pathway of the Small Saphenous Vein (SSV) [3].	7
Figure 2.4	The illustration shows how a varicose vein forms in a leg. Figure A shows a normal vein with a working valve and normal blood flow. Figure B shows a varicose vein with a deformed valve, abnormal blood flow, and thin, stretched walls. The middle image shows where varicose veins might appear in a leg [4].	8
Figure 2.5	Ligation and stripping illustration [5].	10
Figure 2.6	The illustration of EVLA [6].	12
Figure 2.7	Schematic absorption spectra of water (H_2O) and (deoxygenated) hemoglobin [7].	14
Figure 2.8	Biolitec Radial Tip Fiber [8].	15
Figure 2.9	Geometrical sketch of the radial emitting fiber (left) and a bare fiber (right) [9].	16
Figure 3.1	Example of human veins that are used in experiments.	18
Figure 3.2	A: 980-nm Diode Laser (opto power corporation model no: OPC-D010-980-FCPS) B: Controller unit (Teknofil Inc., Istanbul, Turkey).	19
Figure 3.3	Block Diagram of 980-nm Diode Laser.	19
Figure 3.4	LabView software interface (V 6.1).	20
Figure 3.5	A: 1940-nm Fiber Laser (IPG Photonics TLR-5-1940) B: Controller Unit (Teknofil Inc, Istanbul, Turkey).	21
Figure 3.6	Block Diagram of 1940-nm Fiber Laser.	21
Figure 3.7	LabView Interface (Teknofil Inc., Istanbul, Turkey).	22

Figure 3.8	A: 600 micron bare fiber (Biolitec for diode Laser Fibers; WFBFSF-603-DL); B: Elves Radial Fiber (Biolitec Radial Fiber).	23
Figure 3.9	View of optical setup. A: 1940-nm fiber laser output; B: lens; C: coupling of laser light to optic fiber; D: 600 μm optic fiber; E: xyz alignment tool.	24
Figure 3.10	A: Schematic diagram of the vein which shows measurement points of the inner and outer diameter before laser application; B: The illustration of laser application.	25
Figure 3.11	A: Schematic diagram of the vein which shows measurement points of the inner and outer diameter after laser application; B: In order to detect thermal damage of the laser application, veins are cut longitudinally and photographed.	26
Figure 3.12	Illustration of Histological Procedure Steps.	27
Figure 4.1	The comparison of the inner diameter ratios between 980-nm diode laser at 8W and 10W power with bare and radial fiber. *, ** statistically significant results. (*, $0.01 < p \leq 0.05$; **, $0.001 < p \leq 0.01$, student t-test)	31
Figure 4.2	The comparison of the outer diameter ratios between 980-nm diode laser at 8W and 10W power with bare and radial fiber.	32
Figure 4.3	The comparison of the application duration between 980-nm diode laser at 8W and 10W power with bare and radial fiber. *, *** are statistically significant results (*, $0.01 < p \leq 0.05$; ***, $p \leq 0.001$, student t-test)	32
Figure 4.4	Comparison of energy delivered per centimeter for 980-nm diode laser at 8W and 10W power with bare and radial fiber. *** is statistically significant result (***, $p \leq 0.001$, student t-test).	33
Figure 4.5	The amount of energy needed for 1 mm inner diameter shrinkage with 980-nm diode laser with bare and radial fiber. **, *** are statistically significant results (**, $0.001 < p \leq 0.01$; ***, $p \leq 0.001$, student t-test).	34

- Figure 4.6 The amount of energy needed for 1 mm outer diameter shrinkage with 980-nm diode laser with bare and radial fiber. **, *** are statistically significant results (**, $0.001 < p \leq 0.01$; ***, $p \leq 0.001$, student t-test). 34
- Figure 4.7 The comparison of the inner diameter ratios between 1940-nm diode laser at 2W and 3W power with bare and radial fiber. * is statistically significant result (*, $0.01 < p \leq 0.05$, student t-test). 35
- Figure 4.8 The comparison of the outer diameter ratios between 1940-nm diode laser at 2W and 3W power with bare and radial fiber. * is statistically significant result (*, $0.01 < p \leq 0.05$, student t-test). 35
- Figure 4.9 Comparison of the application duration between 1940-nm fiber laser at 2W and 3W power with bare and radial fiber. *** is statistically significant result ($p \leq 0.001$, student t-test). 36
- Figure 4.10 Comparison of energy delivered per centimeter for 1940-nm fiber laser at 2W and 3W power with bare and radial fiber. 36
- Figure 4.11 The amount of energy needed for 1 mm inner diameter shrinkage with 1940-nm diode laser with bare and radial fiber. 37
- Figure 4.12 The amount of energy needed for 1 mm outer diameter shrinkage with 1940-nm diode laser with bare and radial fiber. 37
- Figure 4.13 Decrease in inner diameter ratios with 980-nm diode laser at 8W and 10W power and 1940-nm Fiber Laser at 2W and 3W power with bare fiber. * is statistically significant result (*, $0.01 < p \leq 0.05$, student t-test). 38
- Figure 4.14 Decrease in outer diameter ratios with 980-nm diode laser at 8W and 10W power and 1940-nm Fiber Laser at 2W and 3W power with bare fiber. 38
- Figure 4.15 Comparison of the application duration between 1940-nm fiber laser at 2W and 3W power and 980-nm diode laser at 8W and 10W with bare fiber. *** is statistically significant results (***, $p \leq 0.001$, student t-test). 39

- Figure 4.16 Comparison of energy delivered per centimeter for 1940-nm fiber laser at 2W and 3W power and 980-nm diode laser at 8W and 10W with bare fiber. *** is statistically significant results (***, $p \leq 0.001$, student t-test). 39
- Figure 4.17 Comparison the amount of energy needed for 1 mm inner diameter shrinkage with 1940-nm fiber laser at 2W and 3W power and 980-nm diode laser at 8W and 10W with bare fiber. *** is statistically significant result (***, $p \leq 0.001$, student t-test). 40
- Figure 4.18 Comparison the amount of energy needed for 1 mm outer diameter shrinkage with 1940-nm fiber laser at 2W and 3W power and 980-nm diode laser at 8W and 10W with bare fiber. **, *** are statistically significant results (**, $0.001 < p \leq 0.01$; ***, $p \leq 0.001$, student t-test). 40
- Figure 4.19 Decrease in inner diameter ratios with 980-nm diode laser at 8W and 10W power and 1940-nm Fiber Laser at 2W and 3W power with radial fiber. Among the laser application groups there is no significant difference. 41
- Figure 4.20 Decrease in outer diameter ratios with 980-nm diode laser at 8W and 10W power and 1940-nm Fiber Laser at 2W and 3W power with radial fiber. Among the laser application groups there is no significant difference. 41
- Figure 4.21 The comparison of the application duration between 1940-nm fiber laser at 2W and 3W power and 980-nm diode laser at 8W and 10W with radial fiber. *** is statistically significant results (***, $p \leq 0.001$, student t-test). 42
- Figure 4.22 Comparison of energy delivered per centimeter for 1940-nm fiber laser at 2W and 3W power and 980-nm diode laser at 8W and 10W with bare fiber. *** is statistically significant results (***, $p \leq 0.001$, student t-test). 42

Figure 4.23	Comparison of the amount of energy needed for 1 mm inner diameter shrinkage with 1940-nm fiber laser at 2W and 3W power and 980-nm diode laser at 8W and 10W with radial fiber. *** is statistically significant result (***, $p \leq 0.001$, student t-test).	43
Figure 4.24	Comparison the amount of energy needed for 1 mm outer diameter shrinkage with 1940-nm fiber laser at 2W and 3W power and 980-nm diode laser at 8W and 10W with radial fiber. *** is statistically significant result (***, $p \leq 0.001$, student t-test).	43
Figure 4.25	The vein layers on histological image.	44
Figure 4.26	Mechanical damages on veins before the laser application. A: Mechanical damage at Tunica Intima, B: Mechanical damage at outside of Tunica Adventitia.	45
Figure 4.27	Histologic images of cross-sectional vein segments which were irradiated by 1940-nm fiber laser with bare and radial fiber.	45
Figure 4.28	Histologic images of cross-sectional vein segments which were irradiated by 980-nm diode laser with bare and radial fiber.	46
Figure 4.29	The comparison of thermal damage according to different fibers. *, ** are statistically significant results (*, $0.01 < p \leq 0.05$; **, $0.001 < p \leq 0.01$, student t-test).	47
Figure 4.30	The comparison of thermal damage according to different wavelengths with radial fiber. *, *** are statistically significant results (*, $0.01 < p \leq 0.05$; ***, $p \leq 0.001$, student t-test).	47
Figure 4.31	The comparison of thermal damage according to different wavelengths with bare fiber. *** is statistically significant results (***, $p \leq 0.001$, student t-test).	48

LIST OF TABLES

Table 3.1	Table shows the experimental groups, laser and optic fiber types were used, at which power the laser was applied and the number of the vein segments that were used in each group.	25
Table 3.2	Tissue Processing Procedure.	28
Table 4.1	The meaning of rank points.	46

LIST OF ABBREVIATIONS

cm	centimeter
EVLA	Endovenous Laser Ablation
GSV	Great Saphenous Vein
H_2O	Water
$H_2O-\mu a$	Water absorption coefficient
<i>Hemoglobin-μa</i>	Hemoglobin absorption coefficient
<i>H&E</i>	Hematoxyline-Eosin
HbO_2	Hemoglobin
<i>Hb</i>	Deoxyhemoglobin
<i>Hz</i>	Hertz
J	Joule
LASER	Light Amplification by the Stimulated Emission of Radiation
mm ²	millimetersquare
<i>ms</i>	milisecond
μm	micrometer
nm	nanometer
RFA	Radiofrequency Ablation
sec	second(s)
SSV	Small Saphenous Vein
Tm:YAP	Thulium Ytterbium Aluminum Phosphate
W	Watt
°C	Celcius degree

1. INTRODUCTION

1.1 Motivation and Objectives

Varicose veins are veins that become enlarged, swollen and twisted due to the venous insufficiency. This is a common problem, arising among adult population assessed in epidemiological studies. Varicose veins generally occur in superficial veins of the legs because of long-time standing or walking. Although serious complications are rare, due to aching, discomfort, edema and muscle cramps, varicose veins decrease quality of life in the people who suffer from varicose veins.

Surgical ligation and stripping of the vessel segments are the traditional treatment for great saphenous venous (GSV) insufficiency. Since being a classical surgery, general anesthesia, scars, post-operative pain, wound infection, saphenous nerve injury and high recurrence rate are the disadvantages of surgical ligation and stripping.

In order to reduce side effects of classical surgical treatment, Endovenous Laser Ablation (EVLA) which is minimally invasive technique have become popular in the treatment of varicose veins. Laser application provides sterile conditions, reduces bleeding and operation time and eliminates the adverse effect of the classical surgery. Moreover, because being minimally invasive technique, there is no need to general anesthesia. However, it has some disadvantages such as nerve damage, skin burn, thrombosis, haematoma at entry site (rare), cellulitis and one case of an arteriovenous fistula that have been reported after EVLA.

In endovenous application, laser light is introduced into the vein lumen by means of a flexible optical fiber via a sheath system. The working principle of EVLA is to deliver laser energy to blood vessel lumen. The laser light is converted into heat depending on laser wavelength used and on the absorption characteristic of the primary target molecules. Thermal shrinkage of collagenous tissue during EVLA plays a sig-

nificant role in the early and late results of the treatment. In clinical treatments, several wavelengths have been proposed; 810, 940 and 980-nm are the most commonly used wavelengths which have high absorption coefficient by hemeoglobin. However, the best treatment parameters are still under investigation to find the optimal energy and wavelength.

The main objective of this study is to investigate new techniques and find the optimal application parameters for Endovenous Laser Ablation. In this study, 1940-nm Tm-fiber laser which has selective energy absorption by water is investigated at different power and compared with the 980-nm diode laser which is generally used in clinical treatment. 1940-nm Tm-fiber Laser is proposed to alternative laser to 980-nm diode laser due to higher absorption by water in the vein tissue. Better absorption may lead to same amount of shrinkage; however, 1940-nm Tm-fiber delivers less energy to patient which results in less pain after treatment. Both 1940-nm Tm-fiber laser and 980-nm diode laser applications were performed with radial and bare fiber in order to compare the different delivery techniques. Bare fiber, which is used during clinical application, delivers the laser light inhomogeneous circumferential and locally focused which leads to high energy fluence and more damage on vein wall. Radial fiber emanates the laser light homogenous circumferential and increases the application area; therefore radial fiber may lead to less thermal damage and increase the patient comfort after laser treatment.

1.2 Outline

In Chapter 2, general information of vein and varicose vein, treatment techniques of varicose veins such as Surgical Ligation and Stripping (Phlebectomy), Endovenous Radiofrequency Ablation, Endovenous Chemical Ablation and Endovenous Laser Ablation are explained.

Chapter 3 gives detailed information about materials used in this study, experimental setup and laser application procedure and Hematoxylin and Eosin staining

methods.

Chapter 4 includes results about laser application and Hematoxylin and Eosin staining procedure.

General discussion of proposed study is given in Chapter 5 and conclusion and future works of the study are given in Chapter 6.

2. BACKGROUND

2.1 Varicose Veins

2.1.1 Structure of the Vein Wall

Veins are blood vessels which transport deoxygenated blood from various region of the body to heart. There are four main types of vein: pulmonary, systemic, superficial and deep veins. Pulmonary veins are large blood vessels that carry oxygenated blood from the lungs to the left atrium of the heart. Deoxygenated blood from the rest of the body is carried to the right atrium of the heart by systemic veins. Superficial veins are not located near a corresponding artery and they are very close to the surface of the skin. In contradiction, deep veins are located close to a corresponding artery and they are located within muscle tissue.

The vein wall consists of three layers (Figure 2.1):

1. Tunica Adventita has a strong outer covering of arteries and veins which contains mostly collagen fibers, connective tissues and elastic fibers. This configuration helps to protect the vein structure and allows the vein to keep away from external trauma.
2. Tunica Media is the middle layer of the veins which is composed of smooth muscles and elastic fibers. The elastic characteristic of the vein helps the vein to elongate which tolerates the changes in blood volume and pressure. Also the narrowing down of the vessels in response to temperature, pressure and trauma is controlled by this layer.
3. Tunica Intima is the inner layer of arteries and veins which is in direct contact with the blood flowing through the vein. This part of the vein consists of smooth endothelial cells. The lumen is the hollow center through which blood flows. This

part of the vein consists of smooth endothelial cells. The lumen is the hollow center through which blood flows. This cell layer has a design that prevents fluids from escaping the vasculature into the tissue. Prostacyclin and nitric oxide which are released from these endothelial cells change vascular tone and regulate blood flow.²

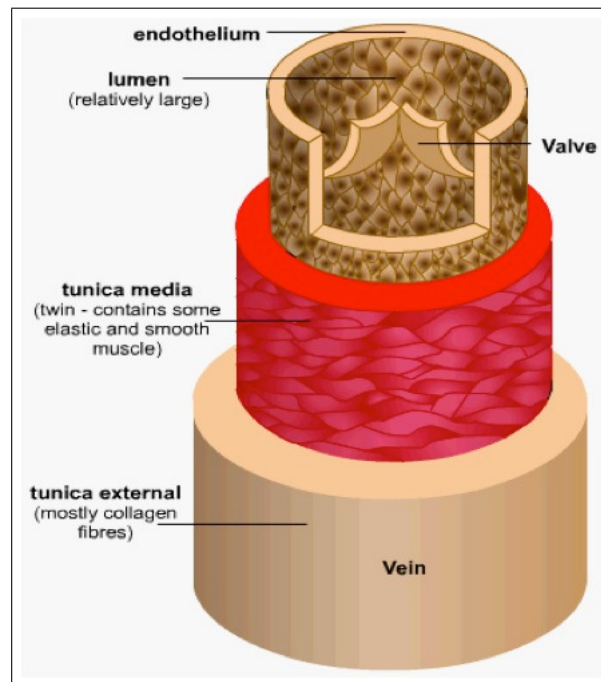


Figure 2.1 The veins consists of three layer: Tunica Adventita, Tunica Media and Tunica Intima. Tunica Intima has valves to keep blood flow in one direction [1].

Also in veins, there are valves in order to prevent any backflow of the blood. Therefore, blood flowing is kept in one direction. Figure 2.2 illustrates the function of the valves in the veins. Muscles are very close to the veins and their contraction and relaxation helps blood movement towards the heart due to valves.

The saphenous veins are two major veins that carry blood from legs to heart. These veins are superficial veins, just below the surface skin tissue and above the muscle layer. There are two types of saphenous vein: Great Saphenous Vein (GSV), which carries blood from ankle to groin and Small Saphenous Vein (SSV), which carries blood from ankle to knee.

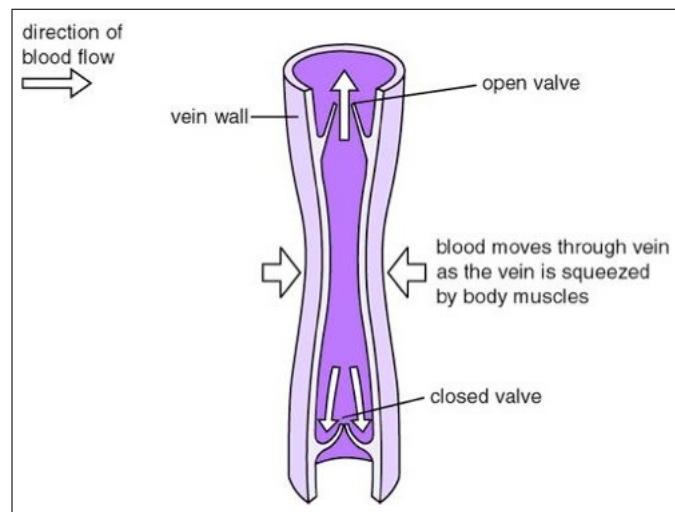


Figure 2.2 The veins consists of three layer: Function of the valves in the veins [2].

2.1.1.1 Great Saphenous Vein (GSV). The GSV, also called as large saphenous vein, starts from the combination of first digit (the large toe) and dorsal venous arch of the foot. It passes from anterior to medial malleolus, then runs from the foot all the way up the medial side of the leg to the saphenous opening. This vein merges to femoral vein at saphenofemoral junction. Figure 2.3.A demonstrates the pathway of the GSV. General pathologies of the GSV are phlebitis, thrombosis, thrombophlebitis and varicose veins. All these diseases typically are not life threatening. GSV can become infected which is called as phlebitis, can experience blockage, which is called thrombosis. Also it can both thrombose and become infected which is called thrombophlebitis. Finally, the GSV is subject to varices which has various treatment options.

2.1.1.2 Small Saphenous Vein (SSV). The SSV, also called as lesser saphenous vein, starts from the combination of the fifth digit (smallest toe) and the dorsal venous arch of the foot. It goes up the back of the leg and merges to popliteal vein which is located in the back of the knee (Figure 2.3.B). Varices, phlebitis, thrombophlebitis and thrombosis are the general diseases of SSV which are similar to GSV.

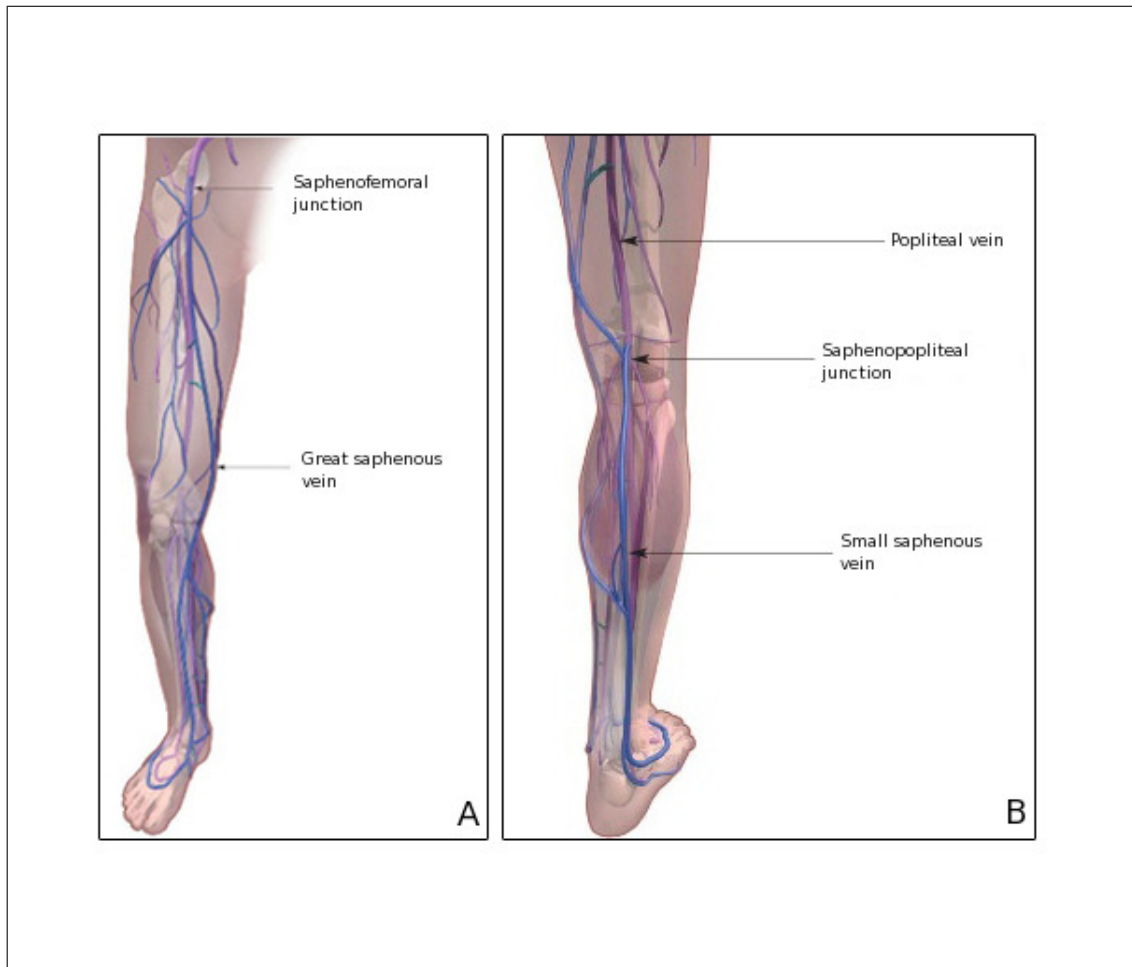


Figure 2.3 A: The pathway of the Great Saphenous Vein (GSV); B: The pathway of the Small Saphenous Vein (SSV) [3].

2.1.2 Structure of Varicose Vein

Varicose veins are common problem, arising in up to 25 % of the adult population assessed in epidemiological studies [10]. In addition to aching, discomfort, edema and muscle cramps, associated complications are eczema, lipo-dermatosclerosis, white atrophy, superficial thrombophlebitis, and venous ulcers [11].

Varicose veins are veins that become enlarged, swollen and twisted. Due to their proximity to the surface of the skin, varicose veins are visible and generally characterized by discolorations. Primarily, varicose veins are found in legs but they can occur other areas of the body. Underlying aetiology and pathogenesis of primary varicose veins remain unclear [12]. Prevalence thought for the underlying problem for

varicose veins is valvular incompetence [13]. In normal veins, veins have valves that prevent the blood from flowing back due to the effect of gravity. When this valves do not work properly, this allow blood to flow back and increase the venous pressure and make vein wall weak which leads to distortion of veins. Figure(2.4) illustrates how a varicose veins form in a leg. However, this hypothesis has been contradicted by the another suggestion that vein wall disorder may lead to valvular incompetence [12].

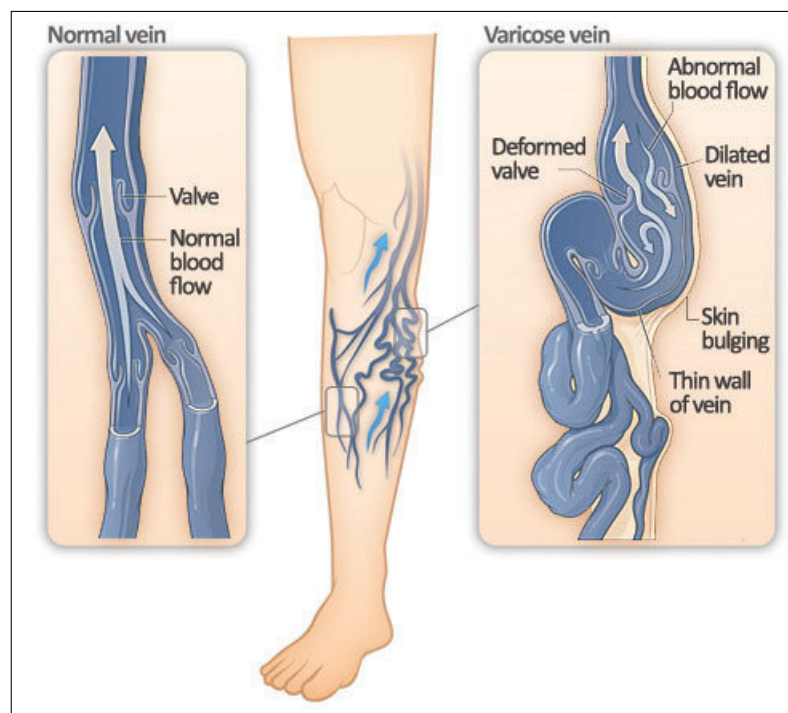


Figure 2.4 The illustration shows how a varicose vein forms in a leg. Figure A shows a normal vein with a working valve and normal blood flow. Figure B shows a varicose vein with a deformed valve, abnormal blood flow, and thin, stretched walls. The middle image shows where varicose veins might appear in a leg [4].

Several factors are supposed to lead to formation of varicose veins such as heredity, age, gender, pregnancy, obesity and lack of movement. Genetic factors raise the risk of varicose vein. People who have varicose veins 21.5 times more likely to have a family members with the problem of varicose veins. Getting older causes the varicose veins due to weakening of calf muscles, reduction in mobility and decrease in components of the veins [12]. Gender factor raises the risk of varicose veins which is more common in women than men [13]. Pregnancy another risk factor for varicose veins. In addition to increase in pressure on the mother' s vein due to growing fetus, upregulation of certain hormones, such as relaxin, oestrogen and progesterone, causes venous relaxation and

increases vein capacitance [12]. Moreover, being overweight puts extra pressure on your veins which can lead to varicose veins. Staying in one position, sitting or standing for a long time can increase the force on your veins and can be a risk factor for the development of varicose vein. In order to regulate blood flowing, the veins need to work harder to pump blood which strain vein valves. Smoking, oestrogen therapy, hypertension and diabetes mellitus have been thought to be another risk factors; however, their roles are still under investigation to be ascertained [12].

2.1.3 Treatment Techniques

All treatment techniques of varicose vein aims to prevent complications and progression of venous insufficiency and improve the cosmetic appearance. Surgical ligation and stripping of Saphenous vein is the classic treatment way of varicose vein; however, the improvement in the technology leads to minimally invasive techniques such as Endovenous Radiofrequency Ablation, Endovenous Chemical Ablation and Endovenous Laser Ablation.

2.1.3.1 Surgical Ligation and Stripping (Phlebectomy). Surgical ligation and stripping of the vessel segments which is sometimes called as Phlebectomy is the traditional treatment for great saphenous venous (GSV) insufficiency which results in varicosities for decades [14]. Surgical tying off the large vein in the leg, great saphenous vein, refers to ligation which is applied to cut off the blood flowing to the varicose veins. The removal of the vein through incisions in the groin or popliteal fossa refers to stripping (Figure 2.5).

General anesthesia is applied during the surgical ligation and stripping. However, recurrence rates after surgery are about 25 % and 50 % at 5 years for the GSV and SSV, respectively. A study with a mean follow-up of 34 years showed recurrence in 60 % of 125 limbs after SFJ ligation and GSV stripping [11]. In addition to recurrence, other disadvantages of the classical surgery is necessity of general anesthesia, bleeding

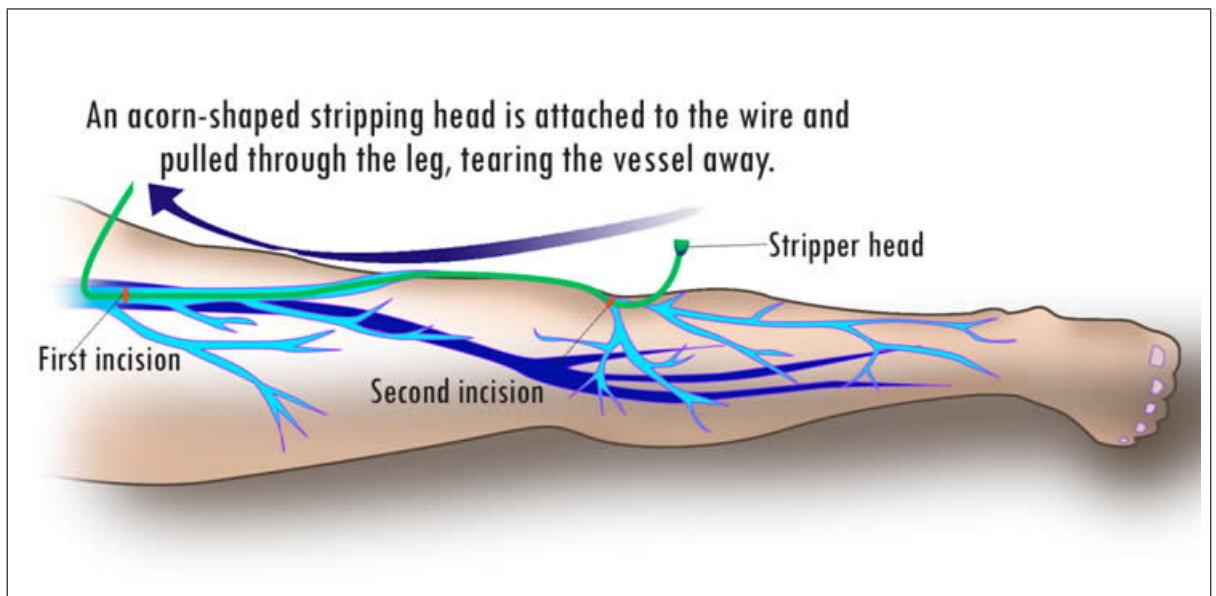


Figure 2.5 Ligation and stripping illustration [5].

and bruising, scars, post-operative pain, long recovery time and adverse events associated with venous stripping such as wound infection and saphenous nerve injury [15]. After surgical ligation and stripping procedure 2 to 4 weeks are needed for recovery [16, 17].

2.1.3.2 Radiofrequency ablation (RFA). Endovenous Radiofrequency Ablation is performed with a catheter emitting bipolar radiofrequency energy which turns into thermal energy to vein lumen. Probe is inserted into the vein and pulled back slowly through the varicose vein. Endovenous catheter generates $85-120\text{ }^{\circ}\text{C}$ heat at the vein wall which leads to heat damage, collagen shrinkage and closure of the target vein. The procedure is performed under the ultrasound imaging guidance with tumescent anesthesia. Compression stockings are applied post operation for several days to 2 weeks. Overall vein closure success of the Radiofrequency Ablation at the range of 89 % at 3 months, 88 % at 1 year, 84 % at 3 years, and 80 % at 5 years [18]. Paresthesia, hematoma, skin burns, infection, bruising, superficial thrombophlebitis, deep venous thrombosis, and pulmonary embolism are the complications that are reported after the Radiofrequency Ablation procedure [19, 20, 21]. After the Radiofrequency Ablation

Procedure, hospitalization and recovery time take 3 to 5 days [22, 20, 23].

2.1.3.3 Endovenous Chemical Ablation. Endovenous chemical ablation is performed by under ultrasound guidance. The catheter is inserted into target segment of varicose vein. The endovenous chemical ablation is performed without local anesthesia. Foam solution which is produced by the combination of air or carbondioxide and chemical sclerosant (polidocanol, sodium morrhuate, or sodium teradecyl sulfate [STDS]). This solution is injected to vein via endovenous catheter under ultrasound guidance, at the same time compressing the saphenofemoral or saphenopopliteal junction in order to eliminate microbubble entrance from solution to deep venous system. While the injected foam is delivered to the distal tributaries via message, the leg is elavated 45 degrees. After the application compression stockings are applied. The foam solution displaces the blood in the treated vein, causing to sclerosis and obliteration of the varicose veins in 1 to 6 weeks [24]. In literature, overall closure of the treated vein is in the range of 82 % at 3 months, 81 % at 1 year, 77 % at 3 years, and 74 % at 5 years [24, 18]. Mild to moderate pain, hyperpigmentation, superficial thrombophlebitis, deep venous thrombosis, pulmonary embolus, hematoma, skin necrosis, transient neurologic events, and rarely major neurologic events in patients with a patent foramen ovale are the complications of the endovenous chemical ablation [25, 19, 26, 27]. After the procedure, patients can return their normal activity within 24 hours. The recurrence rate of the endovenous chemical ablation is higher than conventional surgery and other thermal endovenous application techniques [28].

2.1.3.4 Endovenous Laser Ablation. The Endovenous Laser Ablation (EVLA) has become popular as a minimally invasive technique for venous insufficiency. When EVLA is compared with traditional ligation plus stripping, the success rate of the EVLA is over 90% after several years of follow-up studies and has less complication rate [29]. During clinical EVLA applications, laser light is delivered into the vein wall via flexible optical fiber under Doppler Ultrasound guidance (Figure 2.6).

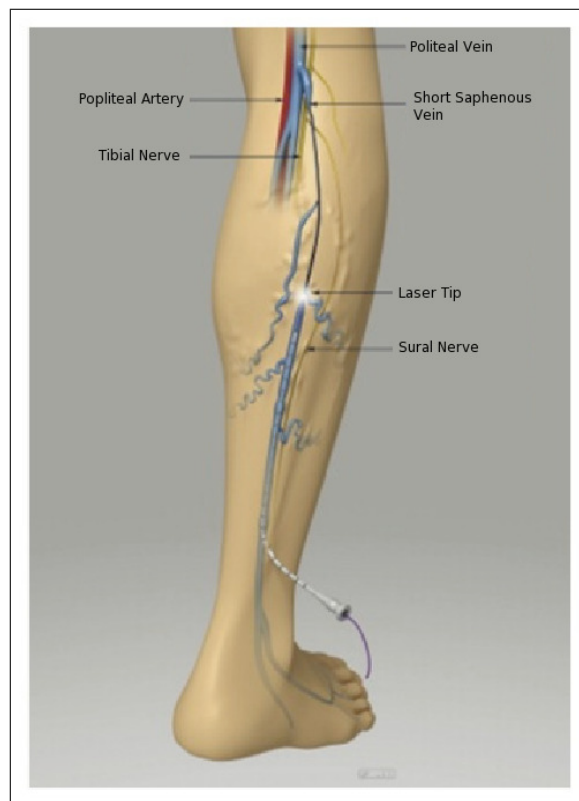


Figure 2.6 The illustration of EVLA [6].

Temperature of the laser tip increases up to $800 \pm \frac{1}{2}^{\circ}\text{C}$ which damages the adjacent tissue during application [15]. Therefore, local anesthesia should be used along the entire length of the varicose vein either manually or with an infusion pump under ultrasound guidance. Tumescent anesthesia is a local anesthesia fluid which is used currently practices to compresses and reduces the diameter of the veins and being protective barrier to minimizes the risk of heat related damage to adjacent tissues [30]. It is also used for separation of vein to be treated from surrounding structures [31].

The mechanism of action of EVLA is still under investigation in order to find out the laser energy emanates from fiber tip absorbed by blood or/and vein wall [32]. There are two theories: steam bubble theory and the direct conduct theory. Proebstle *et al* investigated steam bubble theory and stated that the heat at the tip of laser fiber leads to formation of steam bubbles from boiling blood which causes thermal shrinkage of collagenous tissue and occlusion of the vessel through thrombus formation [33]. The 6 mm diameter blood filled silicon was used and EVLA was applied with increasing

pulsed dose energy. The steam which was generated post application was collected and quantified. It is found that 15 J pulse energy caused to formation of 6mm diameter steam bubble which is equal to 170 mm^3 volume of steam [34]. However, Rox Anderson *et al* proposed that bubble steam theory fails to explain the quantity of energy delivery to the vein during EVLA and carbonization phenomena. At atmospheric pressure, converting 1 mm^3 of water to 1700 mm^3 steam requires 2.5 J of energy. Therefore, $10,200 \text{ mm}^3$ of steam should be produced by 15 J of energy at the 100 % efficiency; thus, 170 mm^3 bubble which Proebstle *et al* found during their experiment, is 1.6 % of the 15 J of energy that was delivered during the application. Carbonization at the fiber tip occurs at about $300 \text{ }^\circ\text{C}$ and regardless of the wavelength used, so light penetration into tissue decreases [31]. Mordon, Zimmet, and Fan and Rox Anderson proposed that laser energy which is absorbed by blood is insufficient to damage the vein wall; therefore, this theory can not be the only mechanism to damage the vein lumen [32, 35, 34]. Moreover, carbonization in the vein wall seen by histological studies proves the direct contact between laser tip [36]. Consequently, light absorption by the vein wall would be the main mechanism for EVLA [32].

The best treatment parameters are still under investigation to find the optimal energy and wavelength. In the literature, the 808-nm, 810-nm, 940-nm, and 980-nm, 1064-nm, 1320-nm, and 1470-nm lasers are used for EVLA. Among these wavelengths, 810-nm, 940-nm, and 980-nm lasers are performed more commonly because they are absorbed by deoxygenated hemoglobin and the 980 nm also by water [4, 8, 6]. 810-nm laser has a high absorption coefficient by hemoglobin ($\text{Hemoglobin-}\mu\text{a}=4 \text{ cm}^{-1}$) and it is also absorbed by the water ($\text{H}_2\text{O-}\mu\text{a}=0,023 \text{ cm}^{-1}$). 980-nm is absorbed both water ($\text{H}_2\text{O-}\mu\text{a}=0,43 \text{ cm}^{-1}$) and hemoglobin ($\text{Hemoglobin-}\mu\text{a}=2 \text{ cm}^{-1}$); however, its water absorption coefficient is higher than 810-nm. At these wavelengths, power is usually set between 10 and 15 W [30]. Longer wavelengths ($>1000 \text{ nm}$) has higher water absorption and are less absorbed by blood than shorter wavelengths, so longer wavelengths may have different and positive effect on EVLA. Figure 2.7 illustrates absorption coefficient of water and biological materials; hemoglobin (HbO_2) and deoxyhemoglobin (Hb). Hemoglobin and deoxyhemoglobin absorb increasingly less light towards the near infrared and dropping out beyond the wavelengths of 800-nm. Water absorption

risers dramatically as one goes farther into infrared, peaking around $3 \mu\text{m}$. [7].

In literature, 1470-nm diode laser which has high water absorption is safe, efficient therapy option and high occlusion rate [37]. In a study of S. Doganci *et al*, 1470-nm laser and radial fiber system reduces the pain, induration, ecchymosis and paraesthesia when it is compared with the 980-nm bare tip laser fiber [38]. In this study, the 1940-nm Thulium Fiber Laser which is a new wavelength fiber laser and has high absorption in water and consequently in the vessel lumen, is used. Although 980-nm diode laser is used for endovenous laser ablation, 1940-nm fiber laser has not been used for this treatment. According to Figure 2.7; 980-nm is absorbed both by water and de-oxygenated hemoglobin. However, 1940-nm is absorbed only by water; it is thought that this wavelength could be successful for this treatment due to water molecules in the vein tissue. In the literature, between 980-nm and 1320-nm wavelength, power is usually performed around 10-15W in most of the applications [36]. Therefore, 8W and 10W were chosen for 980-nm laser. The power of the 980-nm laser is compared with the 1940-nm laser and for 1940-nm fiber laser, the approximate power range was chosen between 2W and 3W.

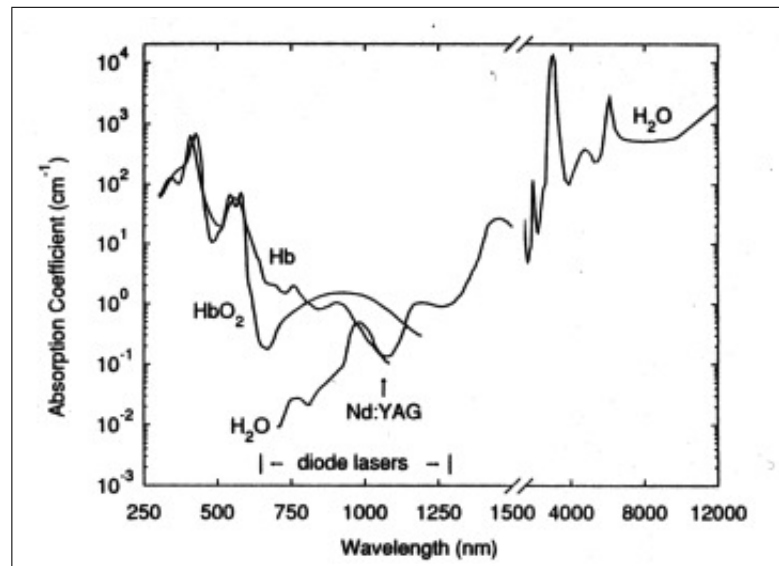


Figure 2.7 Schematic absorption spectra of water (H_2O) and (deoxygenated) hemoglobin [7].

The working principle of the EVLA based on the delivery of the laser light which is converted into heat depending on laser wavelength and absorption characteristics of

the targeted molecules in the blood vessel lumen. Therefore, variety of factors all together influence the vein wall occlusion during the procedure. In addition to this, light distribution within the vessel could affect the procedure. Generally bare and flat cut fibers are used in clinical applications which cause inhomogeneous circumferential light delivery to the vessel wall, so nonuniform tissue change and sometimes perforation are observed. New radial laser fiber tip which emanates laser light homogenous circumferential (360°) is developed (Figure 2.8).

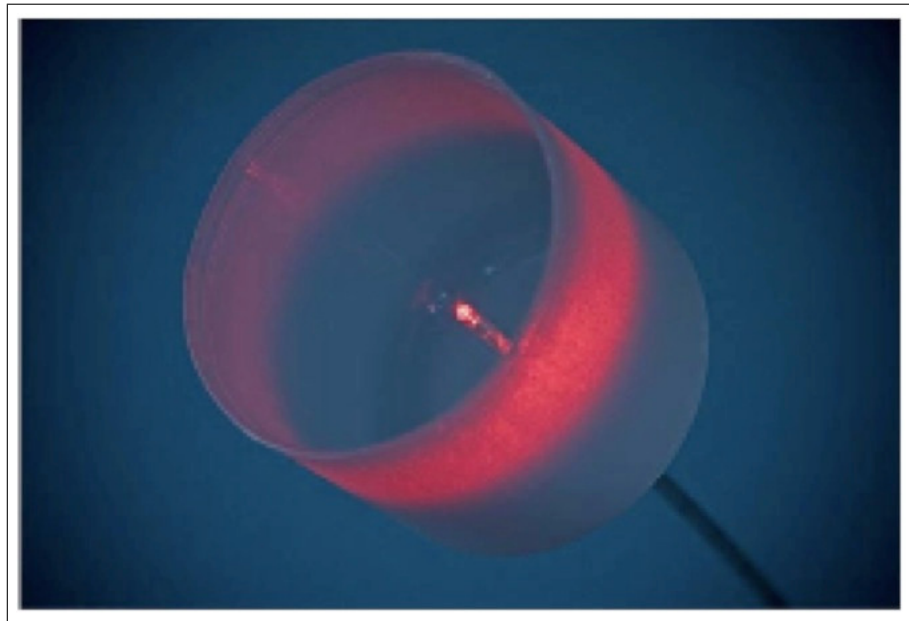


Figure 2.8 Biolitec Radial Tip Fiber [8].

In the vessel Laser irradiation area increases and fluence rate decreases with the radial fiber when it is compared with bare fiber [9]. The geometrical sketch of radial and bare fiber is shown in Figure 2.9. High amount of fluence rate to the tissue ($FR > 1000 \text{ W/cm}$) leads to local perforations [39]. Thus, no perforation could be observed when radial fiber is used [9].

In literature, radial fiber tip is used with water target wavelength (1470-nm) to compare with the bare fiber with 980-nm laser wavelength and as a result radial fiber tip with 1470-nm wavelength is more successful than the latter [38]. However, it is impossible to make a decision about whether the fiber tip or laser wavelength or both of them are effective for this result. Therefore, in this study radial fiber tip is compared

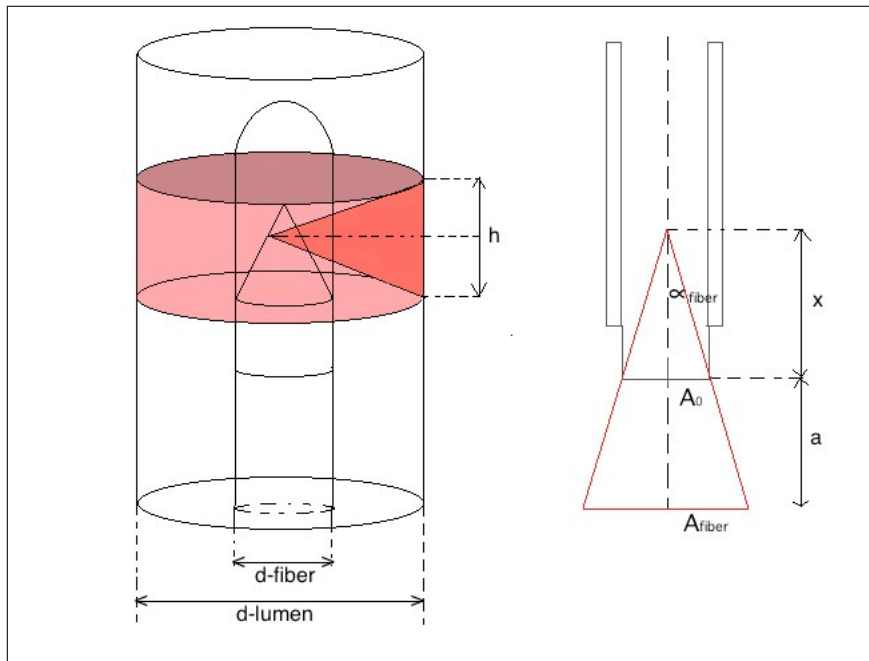


Figure 2.9 Geometrical sketch of the radial emitting fiber (left) and a bare fiber (right) [9].

with the bare fiber tip at same wavelengths (both 980-nm and 1940-nm wavelengths).

Clinical success of EVLA is based on the permanent occlusion of the treated veins, successful removal of varicose veins and returning to normal activity quickly [40]. The recent studies demonstrates that closure rate of the treated vein is 93 % between 3 months and a year and 95 % between 3 and 5 years. It is reported that EVLA is more successful than classical surgery in terms of obliteration and low recurrence rate with the range of 1 % to 5 % [41]. When EVLA is compared with RF, complication rates range between 0 % and %10 after EVLA and between 4 % and 23 % after RF [42]. In addition to complication rates, occlusion rates of the EVLA (98 %-100 %) is slightly higher than the RF (83 %-100 %) [42].

Since being minimally invasive, EVLA is performed under local anesthesia and after application there is no scars, minimal postoperative pain and less recovery time. Since being minimally invasive, people return to their usual life faster than classical surgery. The nerve damage, skin burn, deep venous thrombosis, haematoma at entry site, cellulitis and one case of an arteriovenous fistula are the complications that have

been reported after EVLA [15].

In this study, 1940-nm Thullium Fiber Laser which is a new wavelength fiber laser and has high absorption by water and consequently in the vessel lumen, is proposed as an alternative laser wavelength for EVLA. Better absorption may lead to same amount of shrinkage; however, during 1940-nm diode laser application less energy delivered to patient which leads to less pain after treatment. Coupling the laser light to the optic fiber is not possible for the wavelength longer than 2000-nm; therefore 1940-nm wavelength is the one parameter that have higher water absorption coefficient and be coupled to optic fiber. 1940-nm Tm Fiber Laser has not been used for this treatment, so it is compared with 980-nm diode laser which is frequently used for endovenous laser ablation in clinical treatment. According to Figure 2.7, 980-nm is absorbed both by water and deoxygenated hemoglobin. However, 1940-nm is absorbed only by water; it is thought that this wavelength could be successful for this treatment due to water molecules in the vein tissue. In the literature, between 980-nm and 1320-nm wavelength, power is usually performed around 10-15W in most of the applications [8]. Therefore, 8W and 10W were chosen for 980-nm laser. The maximum output power of 1940-nm fiber laser is 5W and according to pre-experiments 2W and 3W power which have similiar effect as 8W and 10W at 980-nm was choosed . Another criteria which was compared in this paper is delivery technique in terms of thermal damage at vessel wall. Bare fiber which is frequently used in clinical treatment is compared with radial fiber which is a new technology fiber. Bare fiber delivers laser energy inhomogenous and locally focused which is thought that the reason of more perforation and carbonization. On the other hand, radial fiber emanates the laser light circularly to the vein wall. The application area of the laser light increases with the radial fiber; therefore energy fluence decreases which is thought that may lead to less thermal damage on vessel wall.

3. METHODS

3.1 Human Veins

In this study, human veins which are obtained from classical surgery, are used. In order to protect their biological nature, human veins are kept in isotonic solution. All experiments have performed less than 12 hours after the surgery.



Figure 3.1 Example of human veins that are used in experiments.

3.2 Lasers and Fibers

980-nm Diode Laser (Figure 3.2.A) (opto power corporation model no: OPC-D010-980-FCPS, Opto Power, Tuscon, AZ, USA) was used in this study. Controller unit (Figure 3.2.B) was used to control the laser by computer (Teknofil Inc., Istanbul, Turkey). Maximum current for 980-nm diode laser is 35A and maximum output for this laser is 14W. Laser application with 980-nm diode laser at 8W and 10W power was used during experiments. The system provides output through a 1 meter fiberber-optic cable. The laser light was coupled to 600-micron laser fiber via SubMiniature version

(SMA) connector (Figure 3.3).

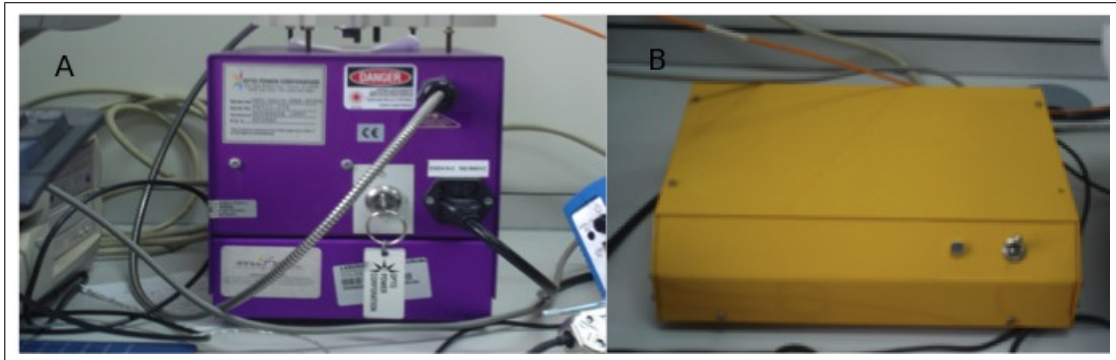


Figure 3.2 A: 980-nm Diode Laser (opto power corporation model no: OPC-D010-980-FCPS) B: Controller unit (Teknofil Inc., Istanbul, Turkey).

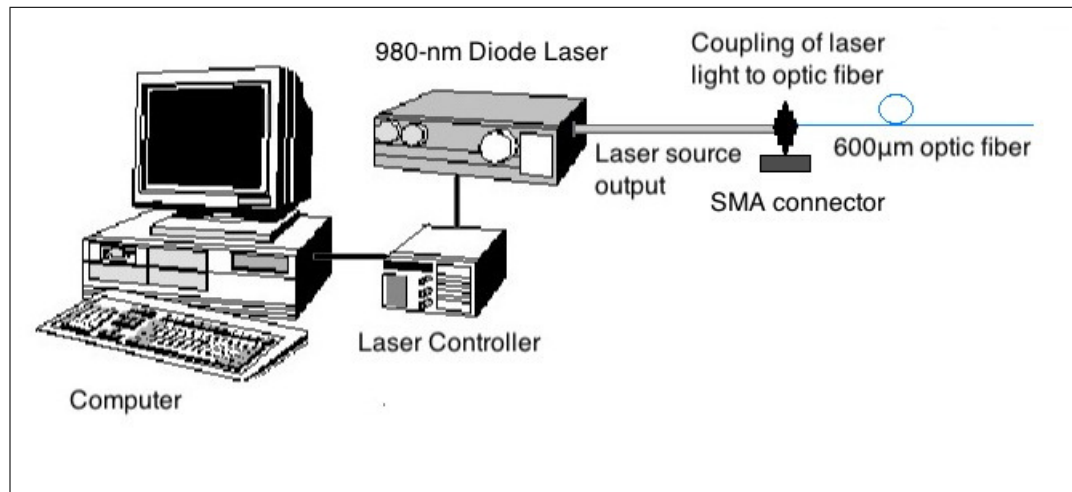


Figure 3.3 Block Diagram of 980-nm Diode Laser.

LabView software interface (V 6.1) (Figure 3.4) were used to control the laser parameters such as power, exposure time, number of cycles, and on-of duration pulses. Before laser application, all parameters were set. The laser power which is wanted to use during the application is adjusted by setting the current from the current toolbar on the interface. As illustration, when the current is set to 35A, the laser output power is measured as 14W. The mode of the application whether continuous or pulse and duration of the application are set by entering data to the duty-cycle, off-cycle and number of cycles bars. In this study, continuous mode was used, so off-cycle and number of cycles were set to 1 and duty-cycle were set according to estimated duration of the application. On-Off button is used for turning on interface and run button with an arrow figure which is at the left top of the interface starts the application. On-Off

button is used whenever the application is wanted to finish. (On-Off button is green when it is off mode and it is red when it is on mode.) On Period (Measured in ms) bar records the duration of the application.

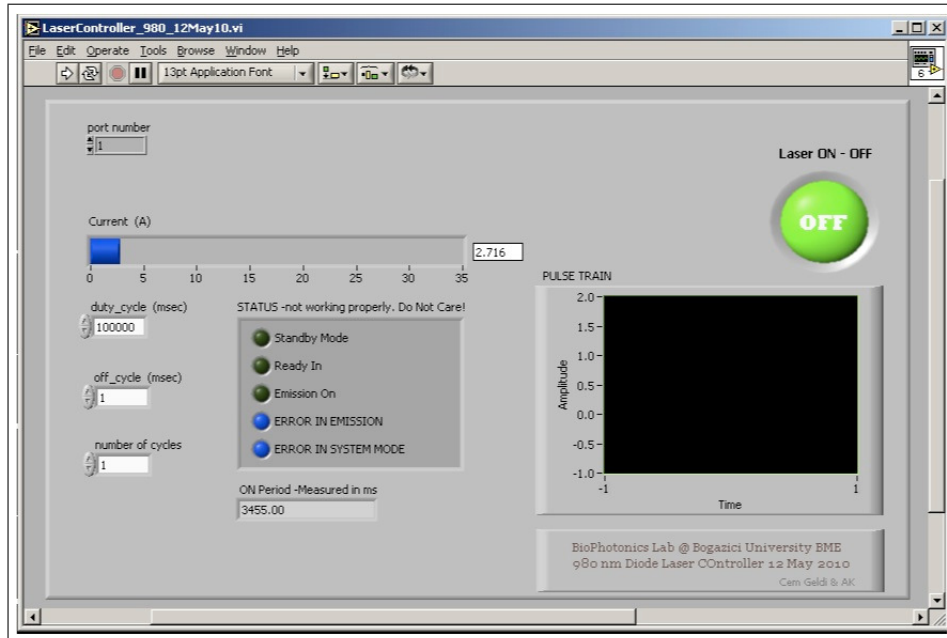


Figure 3.4 LabView software interface (V 6.1).

1940-nm Thullium Fiber Laser (Figure 3.5.A) (IPG Photonics TLR-5-1940) was used with controller unit (Teknofil Inc, Istanbul, Turkey) (Figure 3.5.B) between laser and computer. Maximum output power of the 1940-nm Fiber Laser is 5W and laser application has been performed at 2W and 3W. The system provides output through a 1 meter fiber-optic cable. Laser light is coupled to 600 micrommeter fiber via optical tools such as holder, lenses and xyz alignment tools (Figure 3.6).

The laser parameters (power, exposure time, number of cycles, and on-off duration of pulses) of the laser were adjusted via LabView interface of an external controller (Teknofil Inc., Istanbul, Turkey) (Figure 3.7). Desired Period, Desired Pulse Width and Number of Pulses help to set the duration and mode (continous or pulsed) of the application. Since lenses are used for coupling the laser light to fiber optic, there is some loss of light; therefore laser output power is set to 5W at interface and laser power is set with button on the laser source. After the set of parameters, the application is started with Start Burst button and finished with Stop Burst button. The black panel

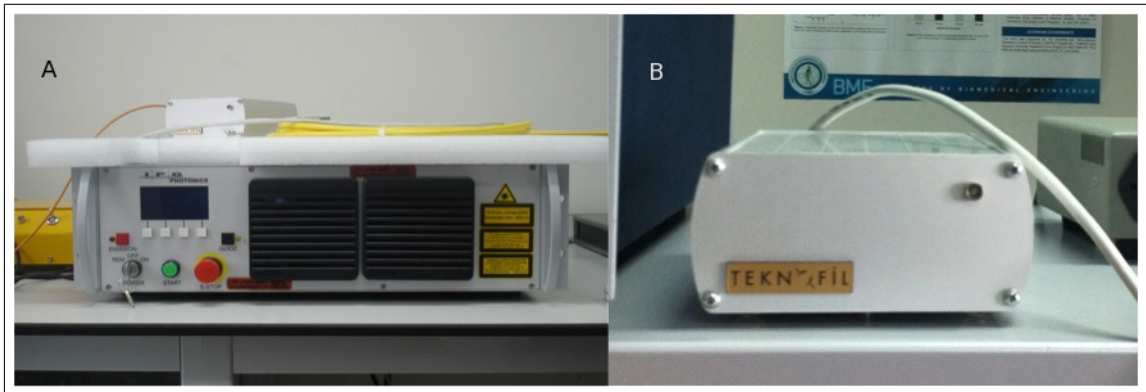


Figure 3.5 A: 1940-nm Fiber Laser (IPG Photonics TLR-5-1940) B: Controller Unit (Teknofil Inc, Istanbul, Turkey).

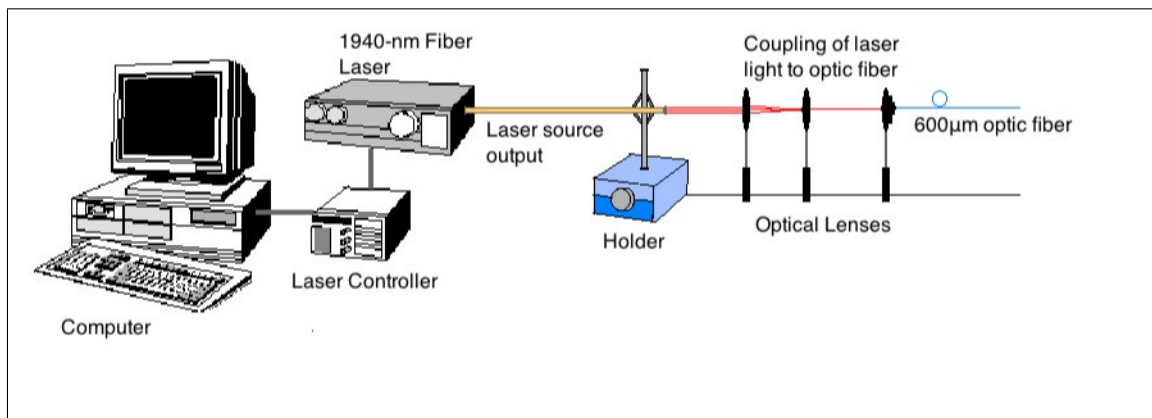


Figure 3.6 Block Diagram of 1940-nm Fiber Laser.

illustrates the laser application duration. Actual Period (ms), Actual Frequency (Hz), Burst Duration (ms), Mean Power (W), Duty Cycle (%), Integral Time (ms), Pulse Energy (mJ) and Burst Energy (J) are recorded and showed after the laser application at the interface.

In this study, 600 micron bare fiber (Biolitec for diode Laser Fibers; WFBFSF-603-DL, Figure 3.8.A) which includes SMA-905 connector on one end and has flat tip on the other end was used. This fiber has no cooling and it is polished. Another fiber that we used in the experiment is Elves Radial Fiber (Biolitec Radial Fiber, Figure 3.8.B) which emits laser light homogenous circumferential (360°).

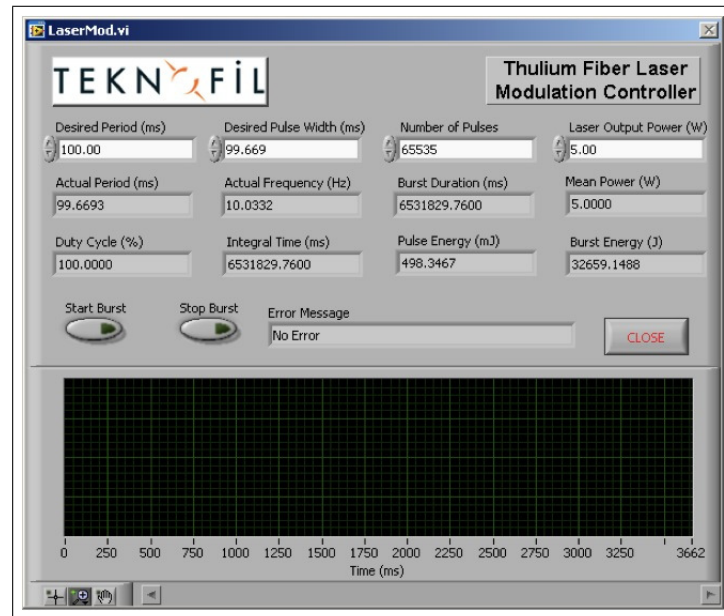


Figure 3.7 LabView Interface (Teknofil Inc., Istanbul, Turkey).

3.3 Laser Application Procedure

In this study, two types of laser and two types of fiber tips were used for irradiation to human veins endovenously to compare their effects at different powers; 980-nm and 1940-nm lasers and fiber tips; bare and radial fiber tips on endovenous laser treatment. The laser light is transferred to 600 μm fiber via optical setup (Figure 3.9).

The output powers were 8 and 10W for 980-nm and 2 and 3W for 1940-nm laser. There are eight main groups which consist of different number of vein segments. Table 3.1 illustrates experimental groups.

Before the application, the fiber tip was cleaved to avoid carbonization effects. The vein segments were cut in 6 cm pieces in length. Before the application, the outer and inner diameters and the length of the vein segments were measured (Figure 3.10.A). The outer diameter was measured at five different points and inner diameter was measured two ends of the vein segment.

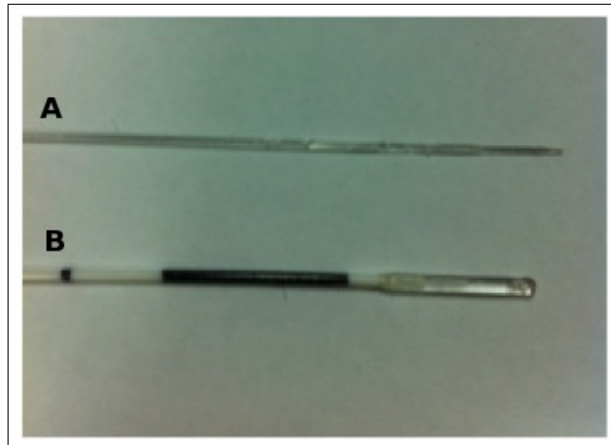


Figure 3.8 A: 600 micron bare fiber (Biolitec for diode Laser Fibers; WFBFSF-603-DL); B: Elves Radial Fiber (Biolitec Radial Fiber).

Each piece was tied with a suture at the proximal end and fastened with needles at both ends. 600-micron laser fiber was inserted from the distal end and vein segments were irradiated with laser starting from the proximal end (Figure 3.10.B). The laser power was adjusted and controlled after every application by power meter (Newport Powermeter Model 1918-C). Laser energy was delivered continuously and the laser fiber was pulled back manually. The time of the application was recorded.

After the application, the outer and inner diameters of the vein segments were measured to compare with measurement before the application to analyze the occlusion (Figure 3.11.A). Again the outer diameter was measured at five different points and inner diameter was measured two ends of the vein segment.

They were cut longitudinally and photographed to observe carbonization effects and thermal damage (Figure 3.11.B).

For eye safety, laser goggles filtering 980-nm and 1940-nm laser light were used during the laser application procedures.

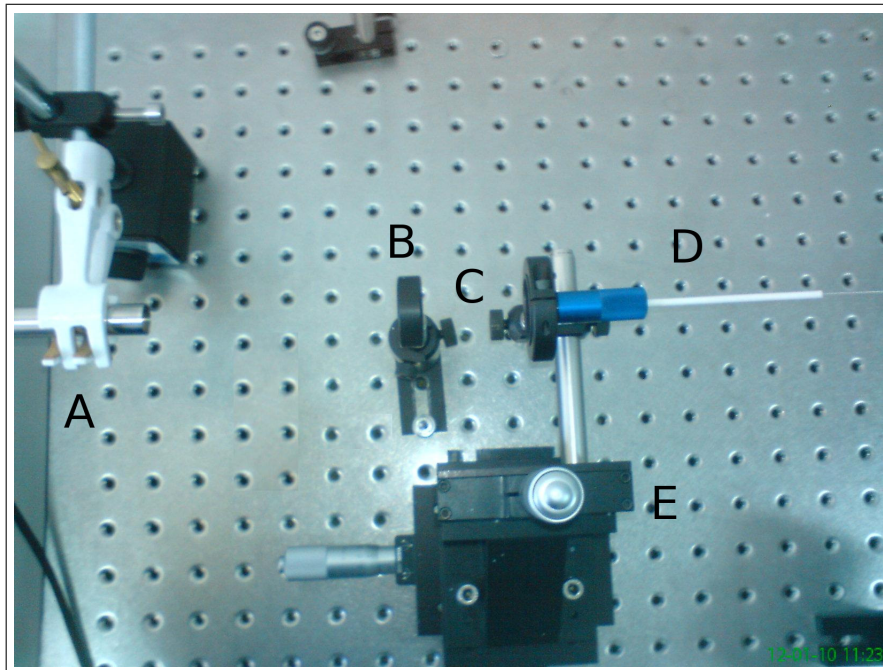


Figure 3.9 View of optical setup. A: 1940-nm fiber laser output; B: lens; C: coupling of laser light to optic fiber; D: 600 μm optic fiber; E: xyz alignment tool.

3.4 Histological Procedure

In order to analyze thermal damage and carbonization effect on vein segments, histological examinations were performed. Tissue processing, paraffin embedding, tissue sectioning and tissue staining with Hematoxyline-Eosin were performed respectively. After all, light microscop was used for taking images (Figure 3.12).

3.4.1 Tissue Processing

After laser application, thermal damage of the vein was checked by histological examination. 10 % PBS-Formaldehyde was used to fix veins after laser application until tissue processing. Tissue processing, the first step of histological procedure, provides dehydration of tissues. The water in the tissue is removed and replaced with a medium that hardens the tissue in order to allow thin sections to be cut by the means of tissue processing. Biological tissue must be supported in a hard matrix which is generally paraffin wax for light microscopy. Since paraffin and water do not get mixed

Table 3.1

Table shows the experimental groups, laser and optic fiber types were used, at which power the laser was applied and the number of the vein segments that were used in each group.

	Groups	Laser Types	Power	Number of Veins
Bare Fiber	1	980-nm	8W	12
	2	980-nm	10W	10
	3	1940-nm	2W	21
	4	1940-nm	3W	22
Radial Fiber	1	980-nm	8W	13
	2	980-nm	10W	14
	3	1940-nm	2W	22
	4	1940-nm	3W	17

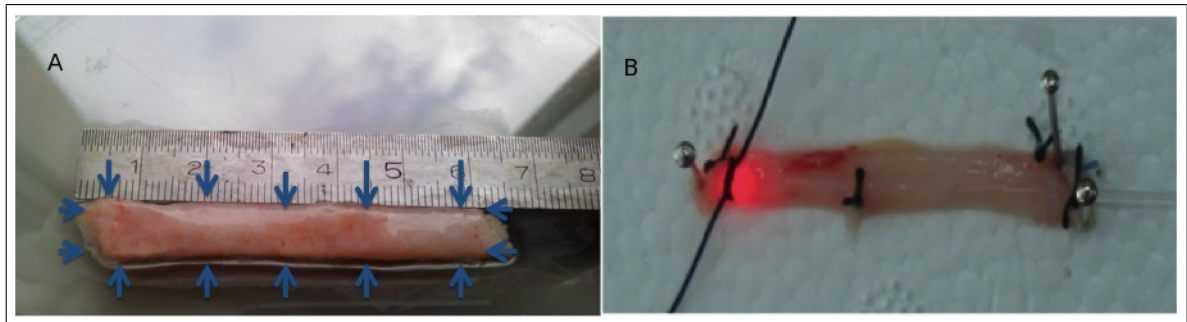


Figure 3.10 A: Schematic diagram of the vein which shows measurement points of the inner and outer diameter before laser application; B: The illustration of laser application.

up together, in the process of dehydration, water, the main constituent of biological tissue must be eliminated from tissue. Tissue dehydration was performed with Alcohol (70 %, 80 %, 90 %, 100 %), Xylene and Paraffin (60 \pm $\frac{1}{2}$ C) by tissue processor (Table 3.2). Concentrated ethanol is used to remove the water; xylene, a hydrophobic clearing agent, helps to remove alcohol and finally molten paraffin wax, the infiltration agent, replaces the xylene. The bath order of tissue is illustrated in Table 3.2.

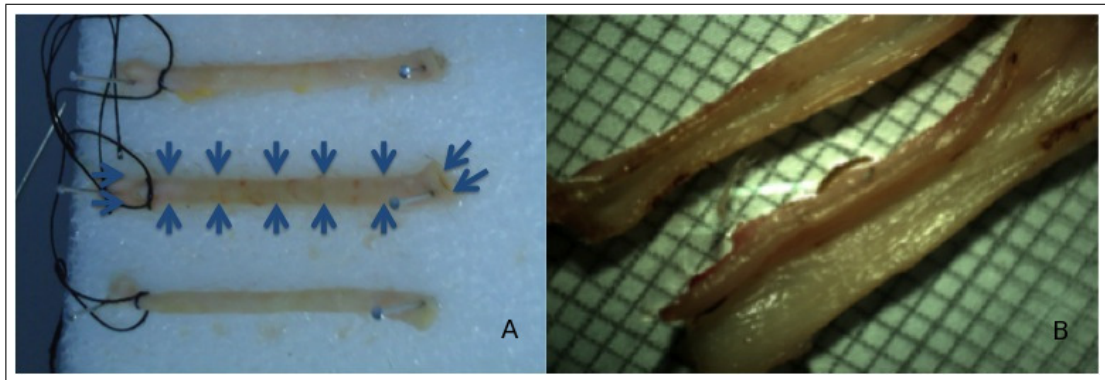


Figure 3.11 A: Schematic diagram of the vein which shows measurement points of the inner and outer diameter after laser application; B: In order to detect thermal damage of the laser application, veins are cut longitudinally and photographed.

3.4.2 Paraffin Embedding

Paraffin embedding provides external embedding after dehydrated, cleared and infiltrated tissues. During this process tissues are positioned into cassettes that are filled with liquid embedding material such as agar, gelatine or wax. After tissues placed into molds, the embedding material is hardened by cooling in the case of paraffin wax. This process was performed with heated paraffin embedding module and cold plate modular tissue embedding system (Leica EG1150C, Germany). The hardened blocks containing the tissue samples are ready to allow thin sections to be cut. Formalin-fixed, paraffin-embedded (FFPE) tissues may be stored for a long time, therefore FFPE tissues are an important resource for historical studies in medicine.

3.4.3 Tissue Sectioning

After vein segments were embedded into paraffin, 10 μm thick cross sectional vein segments were taken by microtome (Leica RM2255, Germany). These sections were put into 40 $^{\circ}\text{C}$ water bath in order to place on glass slides. Then, at 60 $^{\circ}\text{C}$ for 2 hours, vein segments were stayed at incubator.

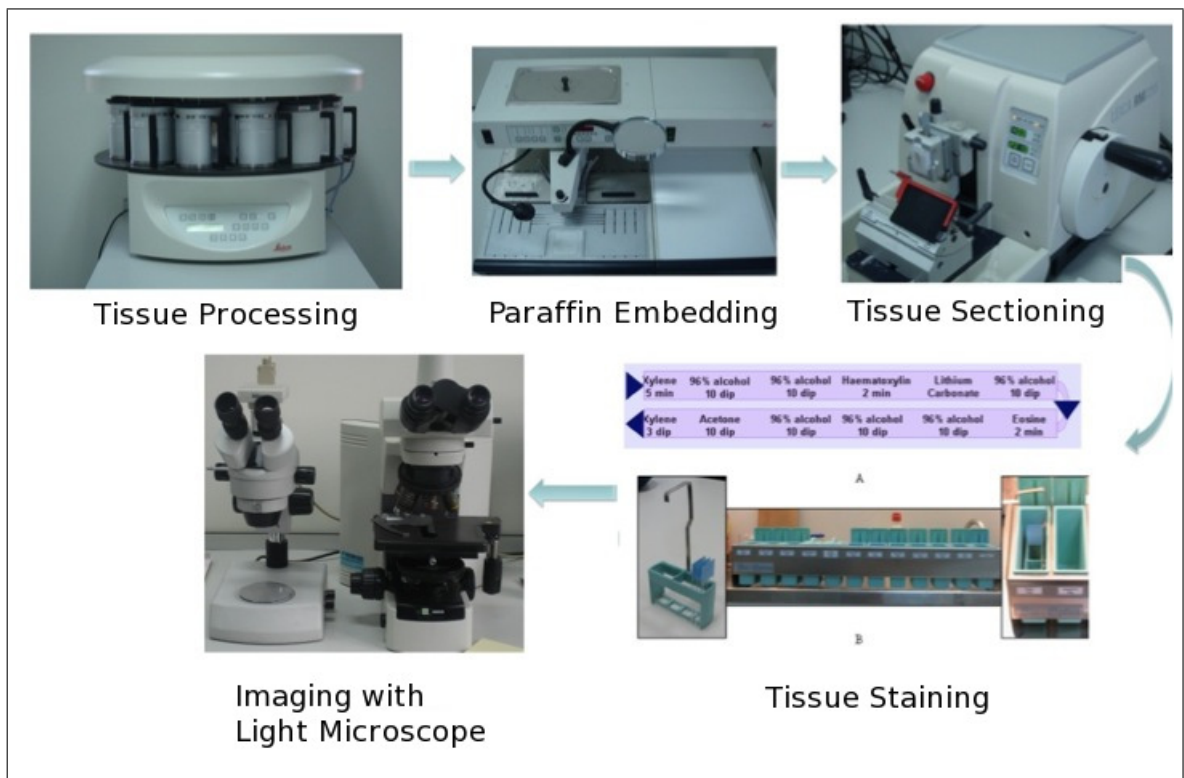


Figure 3.12 Illustration of Histological Procedure Steps.

3.4.4 Tissue Staining

Hematoxyline-Eosin (H&E) Staining, which is a staining method in histology, helps to identify general tissue structure. After embedding in paraffin and tissue sectioning, this process will be performed. The basic dye haematoxylin and alcohol-based acidic eosin Y are two applications for staining method. The basic dye haematoxylin colors basophilic structures with blue-purple hue and alcohol-based acidic eosin Y colors eosinophilic structures bright pink. The basophilic structures are usually the ones containing nucleic acids, such as the ribosomes and the chromatin-rich cell nucleus, and the cytoplasmic regions rich in RNA. The eosinophilic structures are generally composed of intracellular or extracellular protein.

H&E procedure was applied as follow:

Table 3.2
Tissue Processing Procedure.

ALCOHOL	70%	1-h
ALCOHOL	70%	1-h
ALCOHOL	80%	1-h
ALCOHOL	80%	1-h
ALCOHOL	90%	1-h
ALCOHOL	90%	1-h
ALCOHOL	100%	1-h
ALCOHOL	100%	1-h
XYLENE	-	1-h
XYLENE	-	1-h
PARAFFIN	60 °C	1.5-h
PARAFFIN	60 °C	1.5-h

- Cross-sectional vein segments on slides were waited in Xylene for 5 minutes.
- Waited in 96 % Alcohol for 2 minutes.
- Waited in 96 % Alcohol for 2 minutes.
- Washed with tap water.
- Stained with Hematoxylene for 1 minutes.
- Washed with tap water.
- Purpled with Lithium-Carbonate 10 dip.
- Washed with tap water.
- Waited in 96 % Alcohol for 2 minutes.
- Stained with Eosin for 2 minutes
- Waited in 96 % Alcohol for 1 minute.
- Waited in 96 % Alcohol for 1 minutes.

- Waited in Xylene for 2 minutes.

After staining procedure, all slides were covered with Entellan and prepared slides' images were taken by CCD camera. There are nine groups of cross-sectional vein segment slides' image: 980-nm at 8W and 10W with bare and radial fibers; 1940-nm at 2W and 3W with bare and radial fibers and a control group which was not applied laser.

For each group ten images were taken and for all image, the carbonization severity was ranked. Then, thermal damages and carbonization effects of all laser types, laser powers and fiber types were determined.

4. RESULTS

4.1 Laser Application Results

Two types of lasers and fiber tips were compared in this study. Before and after the laser application, inner and outer diameter of the vein was measured. The amount of closure ratio of the vein was calculated by dividing final inner and outer diameters by initial inner and outer diameters. The closure ratio of the inner and outer diameters was compared for different laser parameters.

Laser application duration was recorded during the application to determine operation time which is an important criteria for the operation. Duration of the laser applications was compared for different laser types and fiber types.

In addition to this, delivered laser energy dose per centimeter of vein applied (J/cm) was calculated. This parameter has been referred to as the endovenous fluence equivalent. Energy (J), which was used during the laser application, was calculated by multiplying power (W) and duration (second).

The amount of energy delivered for 1 mm decrease in inner and outer diameter was calculated to determine the laser application which can be performed with less energy. This parameter was obtained by dividing energy to the shrinkage of the vein treated.

Statistical analysis was performed using a two-tailed, unpaired Student's t-test with unequal sample size to determine statistical differences for groups as indicated. Differences with $p \leq 0.05$ were regarded as significant.

4.1.1 980-nm Diode Laser Application with Bare Fiber and Radial Fiber

4.1.1.1 Decrease in Inner and Outer Diameter . Laser application with 980-nm diode laser at 8W and 10W power was performed both bare and radial fiber. According to fiber types, the closure ratio of inner diameter with radial fiber at 8W is significantly more than with bare fiber at 8W ($0.001 < p \leq 0.01$, student t-test). According to increasing power, 980-nm diode laser at 10W power with radial fiber has significantly less closure ratio than 980-nm diode laser at 8W with radial fiber for inner diameter ($0.01 < p \leq 0.05$, student t-test). Analysis found no significant differences between the other groups (Figure 4.1).

The closure rate of outer diameter for 980-nm diode laser at 8W and 10W power with radial and bare fiber have similar results and analysis shows no significant differences between the groups (Figure 4.2).

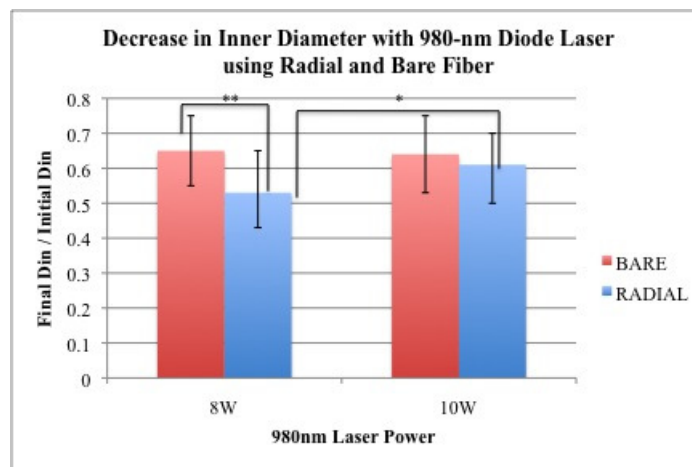


Figure 4.1 The comparison of the inner diameter ratios between 980-nm diode laser at 8W and 10W power with bare and radial fiber. *, ** statistically significant results. (*, $0.01 < p \leq 0.05$; **, $0.001 < p \leq 0.01$, student t-test)

4.1.1.2 Operation Time. The laser radiation was applied to 5 cm vein segments and duration of the application was recorded.

According to Figure 4.3, it is illustrated that duration time becomes shorter with bare fiber.

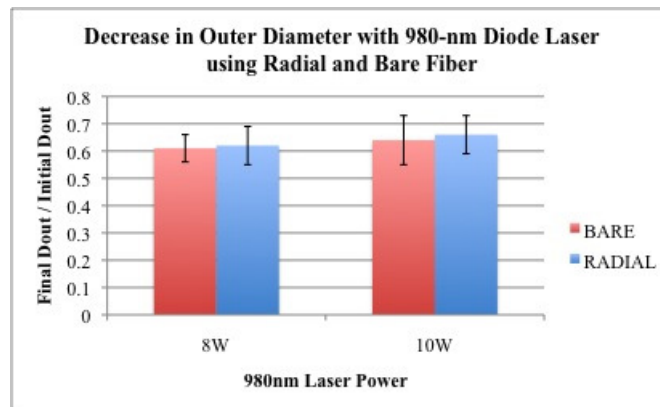


Figure 4.2 The comparison of the outer diameter ratios between 980-nm diode laser at 8W and 10W power with bare and radial fiber.

Analysis shows that 980-nm diode laser application with bare fiber significantly less than the radial fiber both at 8W and 10W power ($p \leq 0.001$, student t-test). Although, there is no important duration difference between bare fiber at 8W and 10W power with bare fiber, the application duration of 980-nm diode laser at 8W significantly shorter than 10W with radial fiber ($0.01 < p \leq 0.05$, student t-test) (Figure 4.3).

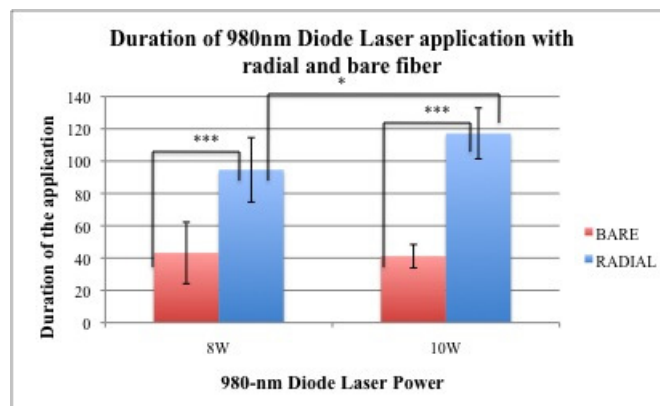


Figure 4.3 The comparison of the application duration between 980-nm diode laser at 8W and 10W power with bare and radial fiber. *, *** are statistically significant results (*, $0.01 < p \leq 0.05$; ***, $p \leq 0.001$, student t-test)

4.1.1.3 Energy per Length. During the application, the fiber tip was pulled back manually according to observation of vein shrinkage. Therefore, every application has different operation duration that affects the used energy during the application.

When delivered energy per centimeter (J/cm) is compared, analysis shows that there is distinct difference between radial fiber and bare fiber at both 8W and 10W power groups ($p \leq 0.001$, student t-test).

According to different power and same fiber, at 8W power with radial fiber energy delivered per centimeter is significantly less than at 10W power with radial fiber ($p \leq 0.001$, student t-test) (Figure 4.4).

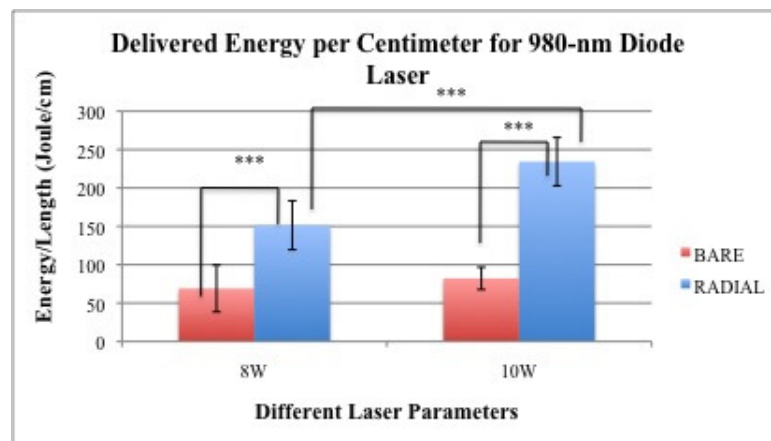


Figure 4.4 Comparison of energy delivered per centimeter for 980-nm diode laser at 8W and 10W power with bare and radial fiber. *** is statistically significant result (***, $p \leq 0.001$, student t-test).

4.1.1.4 The Amount of Energy Delivered for 1 mm Shrinkage. The amount of energy delivered for 1 mm inner diameter shrinkage with 980-nm diode laser is significantly less with bare fiber than radial fiber at 8W ($0.001 < p \leq 0.01$, student t-test). When the power is increased, it is observed that the result is same as low energy result. Distinctly less energy is needed for 1 mm inner diameter shrinkage with bare fiber than radial fiber at 10W ($p \leq 0.001$, student t-test). Energy usage at 8W is significantly less than at 10W with radial fiber ($0.001 < p \leq 0.01$, student t-test) (Figure 4.5).

The amount of energy delivered for 1 mm outer diameter shrinkage with 980-nm diode laser is significantly less with bare fiber than radial fiber at both 8W and 10W ($0.001 < p \leq 0.01$, student t-test). 1 mm shrinkage in outer diameter is obtained with significantly less energy at 8W than 10W with radial fiber during 980-nm diode laser application ($0.001 < p \leq 0.01$, student t-test) (Figure 4.6).

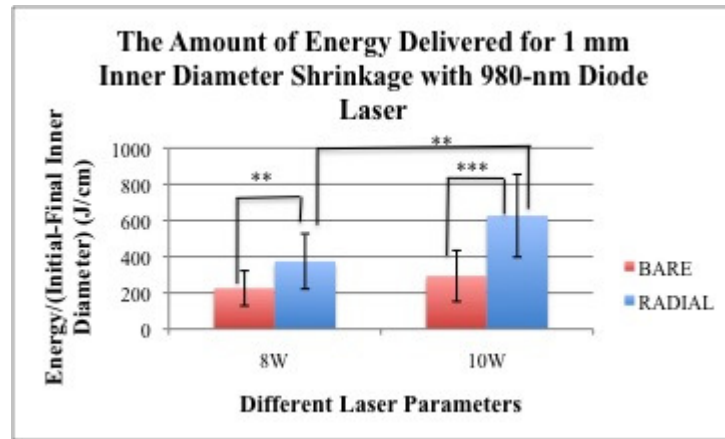


Figure 4.5 The amount of energy needed for 1 mm inner diameter shrinkage with 980-nm diode laser with bare and radial fiber. **, *** are statistically significant results (**, $0.001 < p \leq 0.01$; ***, $p \leq 0.001$, student t-test).

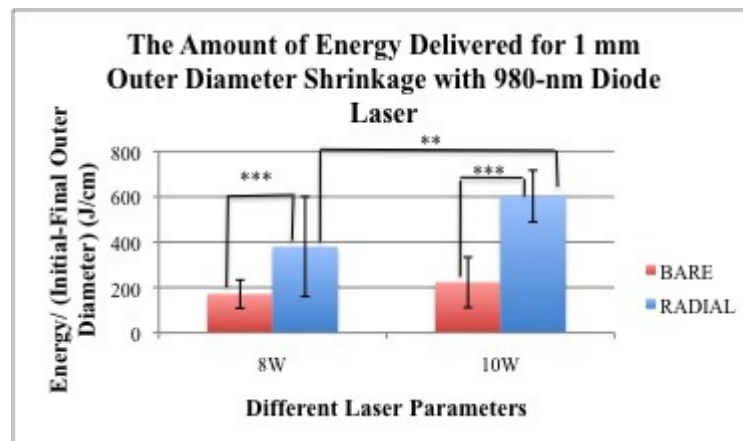


Figure 4.6 The amount of energy needed for 1 mm outer diameter shrinkage with 980-nm diode laser with bare and radial fiber. **, *** are statistically significant results (**, $0.001 < p \leq 0.01$; ***, $p \leq 0.001$, student t-test).

4.1.2 1940-nm Fiber Laser Application with Bare Fiber and Radial Fiber

4.1.2.1 Decrease in Inner and Outer Diameter. Laser application with 1940-nm fiber laser at 2W and 3W power was performed both bare and radial fiber.

According to constant power and changing fiber types, the closure ratio of inner diameter with radial fiber at 3W is significantly more than bare fiber at 3W ($0.01 < p \leq 0.05$, student t-test).

According to same fiber type and different power application, 1940-nm fiber laser at 2W power has significantly higher closure ratio than 3W power with bare fiber for inner diameter ($0.01 < p \leq 0.05$, student t-test). Analysis found no significant differences between the other groups (Figure 4.7).

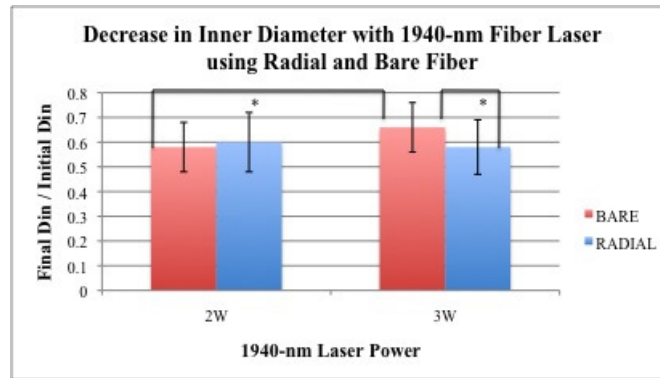


Figure 4.7 The comparison of the inner diameter ratios between 1940-nm diode laser at 2W and 3W power with bare and radial fiber. * is statistically significant result (*, $0.01 < p \leq 0.05$, student t-test).

Laser applications with 1940-nm fiber laser at 2W and 3W power were performed with both bare and radial fiber. The closure ratio of outer diameter with bare fiber at 2W is significantly more than radial fiber at 2W ($0.01 < p \leq 0.05$, student t-test). Among other laser groups, 1940-nm fiber laser at 2W power has significantly higher outer diameter closure ratio than 3W power with bare fiber ($0.01 < p \leq 0.05$, student t-test). Analysis shows that other groups have similar results to each others (Figure 4.8).

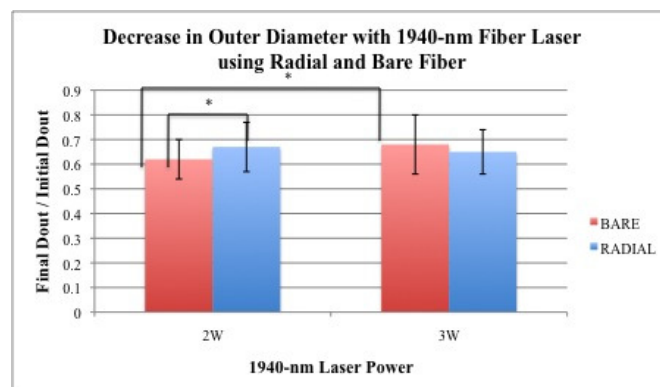


Figure 4.8 The comparison of the outer diameter ratios between 1940-nm diode laser at 2W and 3W power with bare and radial fiber. * is statistically significant result (*, $0.01 < p \leq 0.05$, student t-test).

4.1.2.2 Operation Time. Among the 1940-nm fiber laser application groups with radial and bare, 2W bare fiber group duration is significantly shorter than the 3W bare fiber group ($p \leq 0.001$, student t-test).

There is no statistically significant difference among other groups (Figure 4.9).

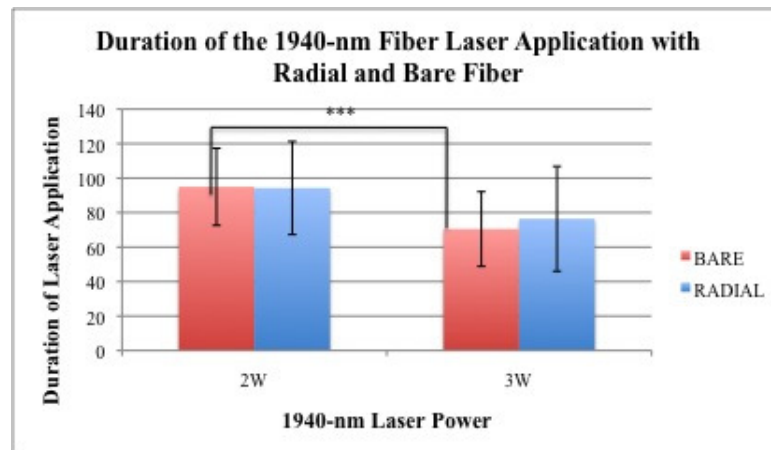


Figure 4.9 Comparison of the application duration between 1940-nm fiber laser at 2W and 3W power with bare and radial fiber. *** is statistically significant result ($p \leq 0.001$, student t-test).

4.1.2.3 Energy per Length. Analysis find no significant differences for delivered energy per centimeter among the 1940-nm fiber laser groups at 2W and 3W with bare and radial fiber (Figure 4.10).

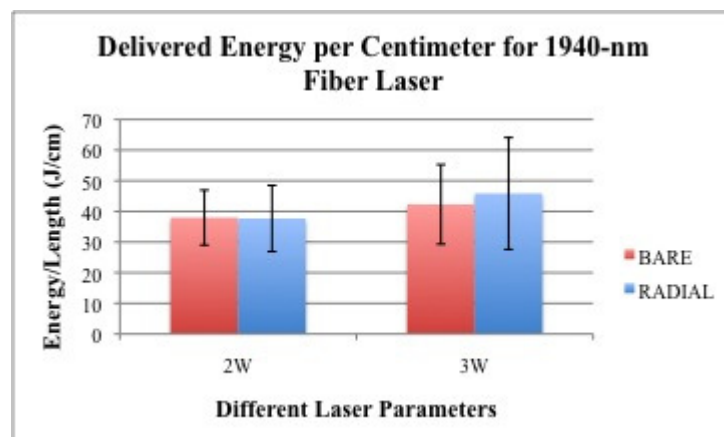


Figure 4.10 Comparison of energy delivered per centimeter for 1940-nm fiber laser at 2W and 3W power with bare and radial fiber.

4.1.2.4 The Amount of Energy Delivered for 1 mm Shrinkage. It is observed there is no significantly difference among 1940-nm fiber laser application groups in terms of the amount of energy delivered for 1 mm decrease in both inner and outer diameter (Figure 4.11, Figure 4.12).

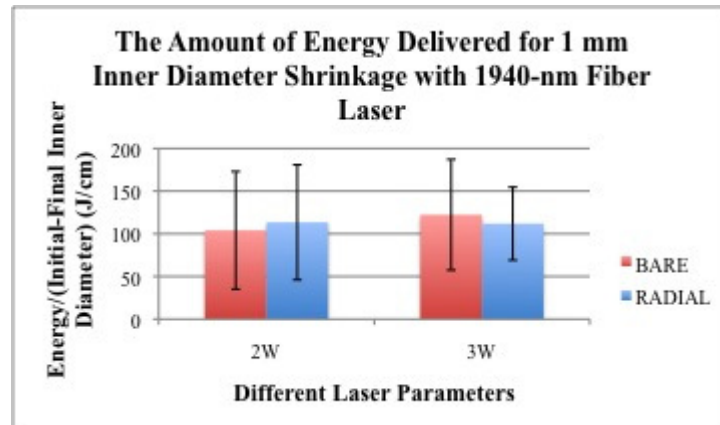


Figure 4.11 The amount of energy needed for 1 mm inner diameter shrinkage with 1940-nm diode laser with bare and radial fiber.

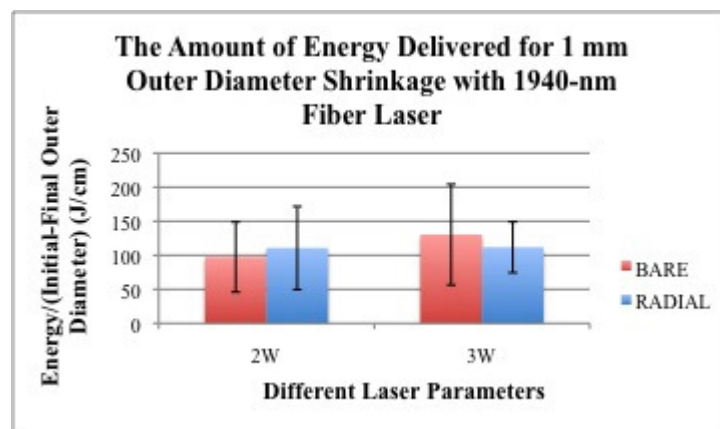


Figure 4.12 The amount of energy needed for 1 mm outer diameter shrinkage with 1940-nm diode laser with bare and radial fiber.

4.1.3 Comparison of 980-nm Diode Laser and 1940-nm Fiber Laser Application with Bare Fiber

4.1.3.1 Decrease in Inner and Outer Diameter. 1940-nm fiber laser at 2W power leads to significantly more decrease in inner diameter than 980-nm diode laser at 8W power ($0.01 < p \leq 0.05$, student t-test).

Among other laser groups there is no distinct difference in inner and outer diameter between 1940-nm fiber laser and 980-nm diode laser (Figure 4.13, Figure 4.14).

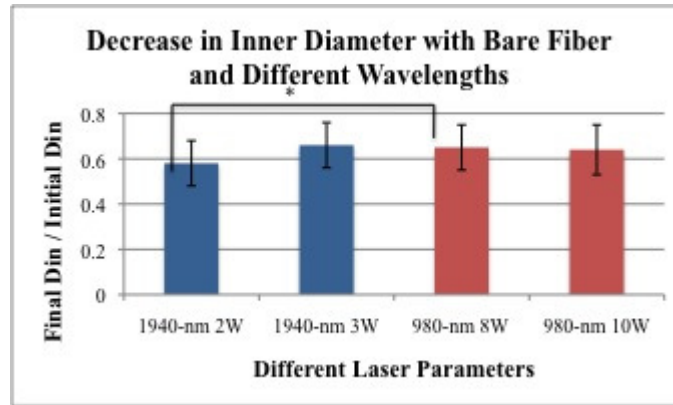


Figure 4.13 Decrease in inner diameter ratios with 980-nm diode laser at 8W and 10W power and 1940-nm Fiber Laser at 2W and 3W power with bare fiber. * is statistically significant result (*, $0.01 < p \leq 0.05$, student t-test).

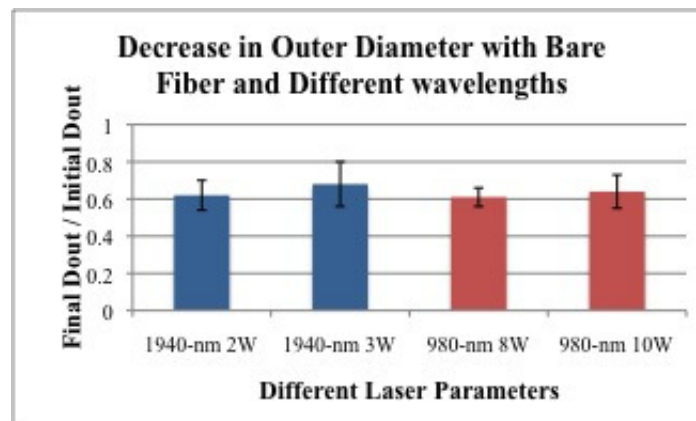


Figure 4.14 Decrease in outer diameter ratios with 980-nm diode laser at 8W and 10W power and 1940-nm Fiber Laser at 2W and 3W power with bare fiber.

4.1.3.2 Operation Time. It is illustrated in Figure 4.15 that the operation time changes with wavelength significantly. The application duration of the 980-nm at 8W is distinctly shorter than the 1940-nm fiber laser at 2W and 3W ($p \leq 0.001$, student t-test). Also, 980-nm at 10W has a shorter application time than 1940-nm fiber laser ($p \leq 0.001$, student t-test) (Figure 4.15).

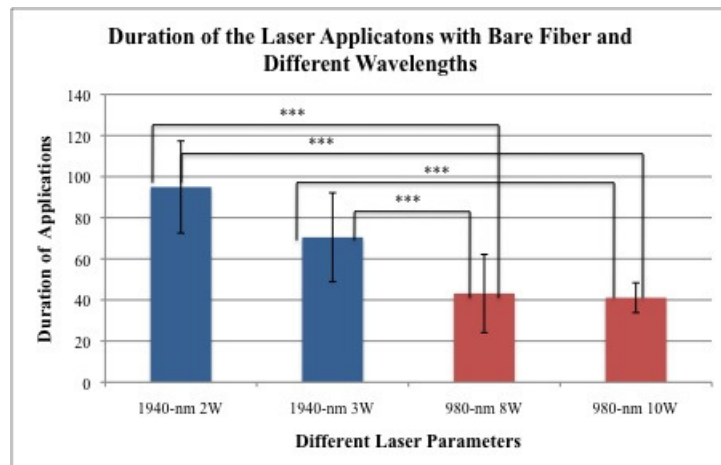


Figure 4.15 Comparison of the application duration between 1940-nm fiber laser at 2W and 3W power and 980-nm diode laser at 8W and 10W with bare fiber. *** is statistically significant results (***, $p \leq 0.001$, student t-test).

4.1.3.3 Energy per Length. The need of energy during the application is compared for 980-nm diode laser and 1940-nm fiber laser. It is observed that longer wavelength needs less energy than the shorter one. At 1940-nm laser application with both 2W and 3W power delivery of energy per length is less than at 980-nm laser application with both 8W and 10W ($p \leq 0.001$, student t-test) (Figure 4.16).

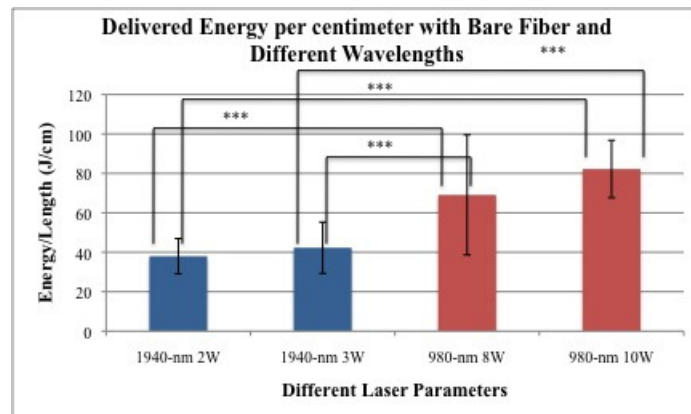


Figure 4.16 Comparison of energy delivered per centimeter for 1940-nm fiber laser at 2W and 3W power and 980-nm diode laser at 8W and 10W with bare fiber. *** is statistically significant results (***, $p \leq 0.001$, student t-test).

4.1.3.4 The Amount of Energy Delivered for 1 mm Shrinkage. 1940-nm fiber laser at both 2W and 3W needs significantly less energy for 1-mm shrinkage in inner diameter than 980-nm diode laser at 8W and 10W with bare fiber application (Figure

4.17).

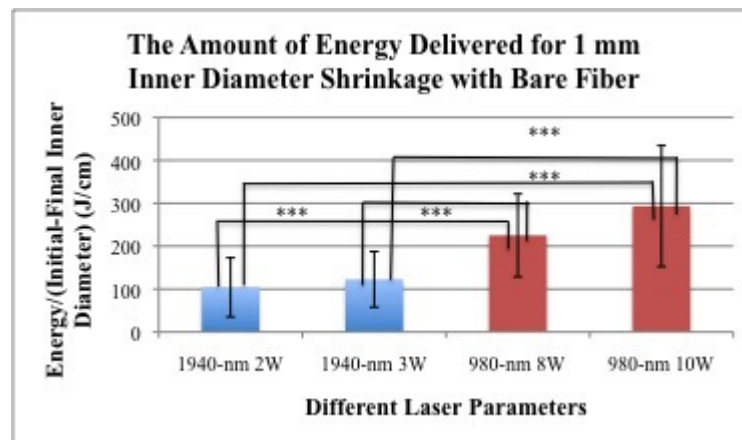


Figure 4.17 Comparison the amount of energy needed for 1 mm inner diameter shrinkage with 1940-nm fiber laser at 2W and 3W power and 980-nm diode laser at 8W and 10W with bare fiber. *** is statistically significant result (***, $p \leq 0.001$, student t-test).

1940-nm fiber laser at 2W needs distinctly less energy for 1 mm outer diameter shrinkage than 980-nm diode laser both at 8W and 10W ($p \leq 0.001$, student t-test). Although 1940-nm 3W has no significant difference with 980-nm at 8W, there is distinct difference between 1940-nm 3W and 980-nm 10W in terms of the amount of energy needed for 1 mm decrease in outer diameter with bare fiber ($0.001 < p \leq 0.01$) (Figure 4.18).

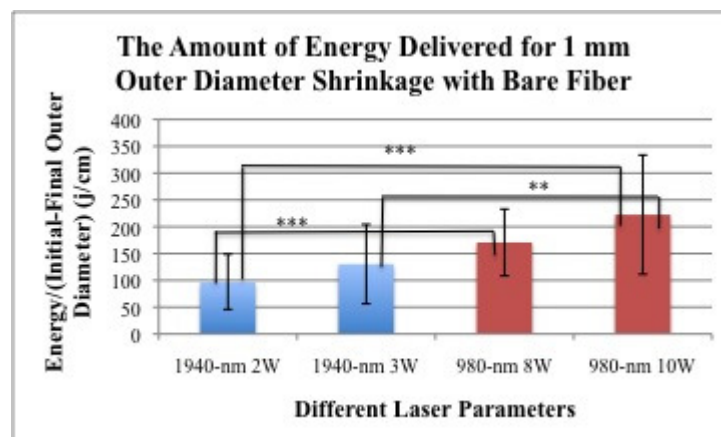


Figure 4.18 Comparison the amount of energy needed for 1 mm outer diameter shrinkage with 1940-nm fiber laser at 2W and 3W power and 980-nm diode laser at 8W and 10W with bare fiber. **, *** are statistically significant results (**, $0.001 < p \leq 0.01$; ***, $p \leq 0.001$, student t-test).

4.1.4 Comparison of 980-nm Diode Laser and 1940-nm Fiber Laser Application with Radial Fiber

4.1.4.1 Decrease in Inner and Outer Diameter. The analysis shows that there is no significant difference in the decrease in both inner and outer diameter between the laser groups of 1940-nm at 2W-3W and 980-nm at 8W-10W (Figure 4.19, Figure 4.20).

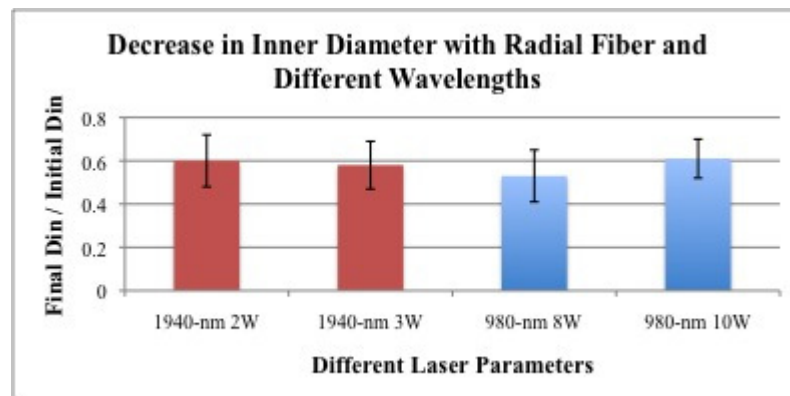


Figure 4.19 Decrease in inner diameter ratios with 980-nm diode laser at 8W and 10W power and 1940-nm Fiber Laser at 2W and 3W power with radial fiber. Among the laser application groups there is no significant difference.

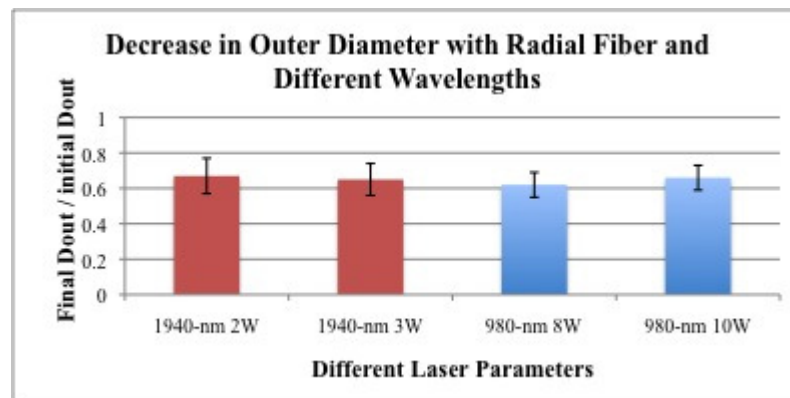


Figure 4.20 Decrease in outer diameter ratios with 980-nm diode laser at 8W and 10W power and 1940-nm Fiber Laser at 2W and 3W power with radial fiber. Among the laser application groups there is no significant difference.

4.1.4.2 Operation Time. The most significantly different operation time result is analyzed between 1940-nm fiber laser at 3W and 980-nm diode laser at 10W ($p \leq 0.001$, student t-test). 1940-nm laser application at 3W power has the shortest application

duration. Also, 1940-nm at 2W laser application duration is distinctly less than 980-nm 10W ($p \leq 0.001$, student t-test). There are no distinct differences between 1940-nm 2W and 980-nm 8W; and 1940-nm 3W and 980-nm 8W (Figure 4.21).

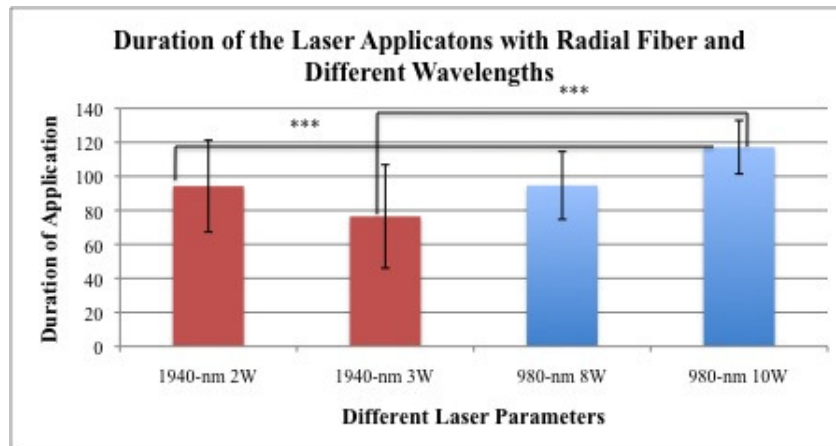


Figure 4.21 The comparison of the application duration between 1940-nm fiber laser at 2W and 3W power and 980-nm diode laser at 8W and 10W with radial fiber. *** is statistically significant results (***, $p \leq 0.001$, student t-test).

4.1.4.3 Energy per Length. The energy needed for the 1940-nm fiber laser application is distinctly less than 980-nm diode laser application groups. It is observed that the delivered energy per centimeter increases with increasing power. Both 2W and 3W at 1940-nm fiber laser needs significantly less energy than 8W and 10w at 980-nm diode laser ($p \leq 0.001$, student t-test) (Figure 4.22).

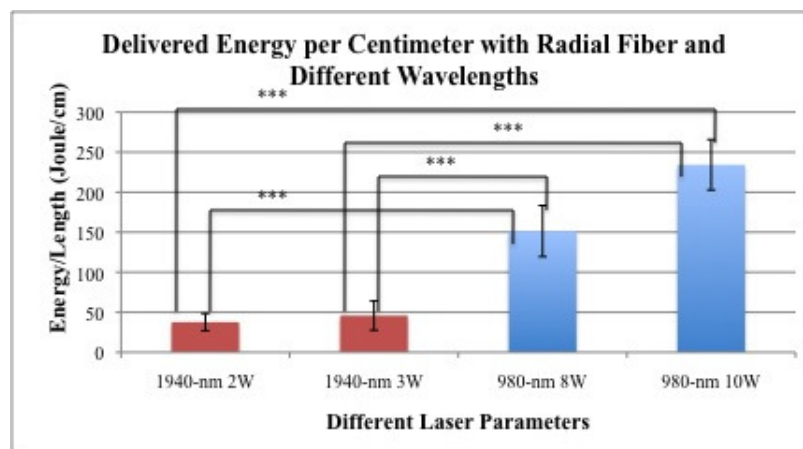


Figure 4.22 Comparison of energy delivered per centimeter for 1940-nm fiber laser at 2W and 3W power and 980-nm diode laser at 8W and 10W with bare fiber. *** is statistically significant results (***, $p \leq 0.001$, student t-test).

4.1.4.4 The Amount of Energy Delivered for 1 mm Shrinkage. The amount of energy delivered for 1 mm decrease in inner diameter with 1940-nm fiber laser both at 2W and 3W is significantly less than with 980-nm diode laser both at 8W and 10W ($p \leq 0.001$, student t-test) (Figure 4.23).

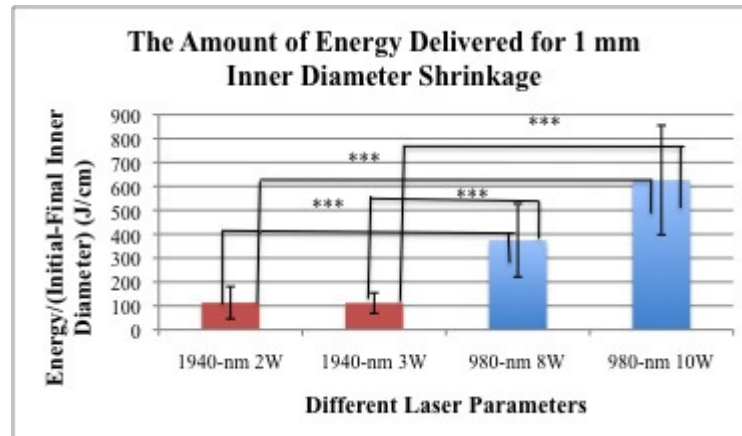


Figure 4.23 Comparison of the amount of energy needed for 1 mm inner diameter shrinkage with 1940-nm fiber laser at 2W and 3W power and 980-nm diode laser at 8W and 10W with radial fiber. *** is statistically significant result (***, $p \leq 0.001$, student t-test).

The amount of energy delivered for 1 mm decrease in inner diameter with 1940-nm fiber laser both at 2W and 3W is significantly less than with 980-nm diode laser both at 8W and 10W ($p \leq 0.001$, student t-test) (Figure 4.24).

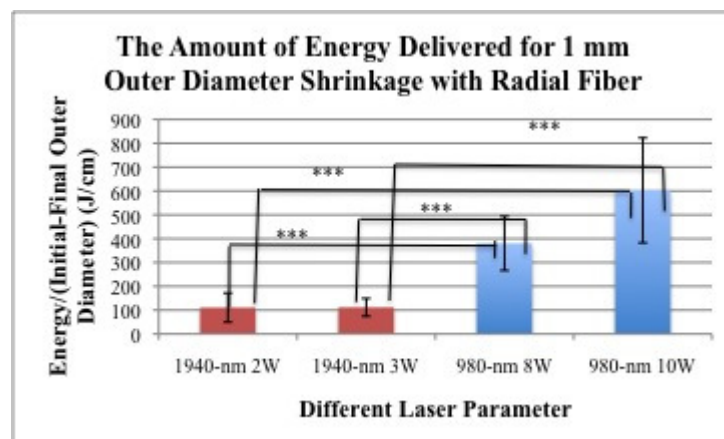


Figure 4.24 Comparison the amount of energy needed for 1 mm outer diameter shrinkage with 1940-nm fiber laser at 2W and 3W power and 980-nm diode laser at 8W and 10W with radial fiber. *** is statistically significant result (***, $p \leq 0.001$, student t-test).

4.2 Histological Procedure Results

For histological examination, there were nine groups: 980-nm at 8W and 10W with bare and radial fibers; 1940-nm at 2W and 3W with bare and radial fibers and a control group. Control group illustrates the vein structure before the laser application. For all groups, 12 images were taken by CCD camera.

Thermal damage severity was determined according to layer of vein where damage occurs; Tunica Intima, Tunica Media or Tunica Adventitia (Figure 4.25).

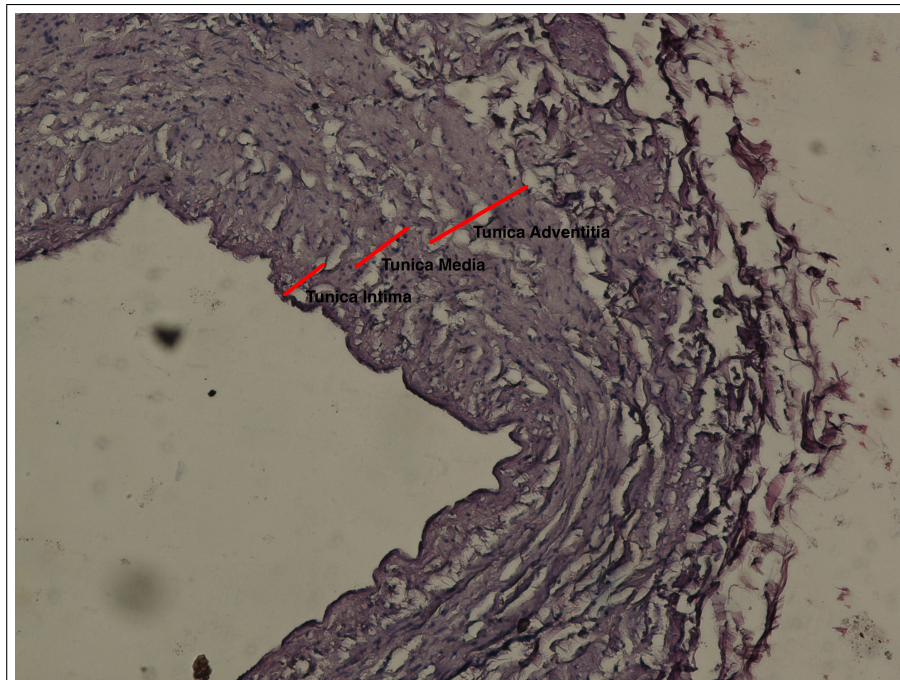


Figure 4.25 The vein layers on histological image.

It is observed that veins that had come from surgical treatment, had mechanical damages at Tunica Intima and outside of the Tunica Advantitia (Figure 4.26).

It is observed from light microscope images that 1940-nm 2W and 3W laser application with radial fiber have close effect. Both of them have damages on Tunica Intima. However with the usage of bare fiber damages on Tunica Intima increases with 1940-nm 2W and 3W (Figure 4.27).

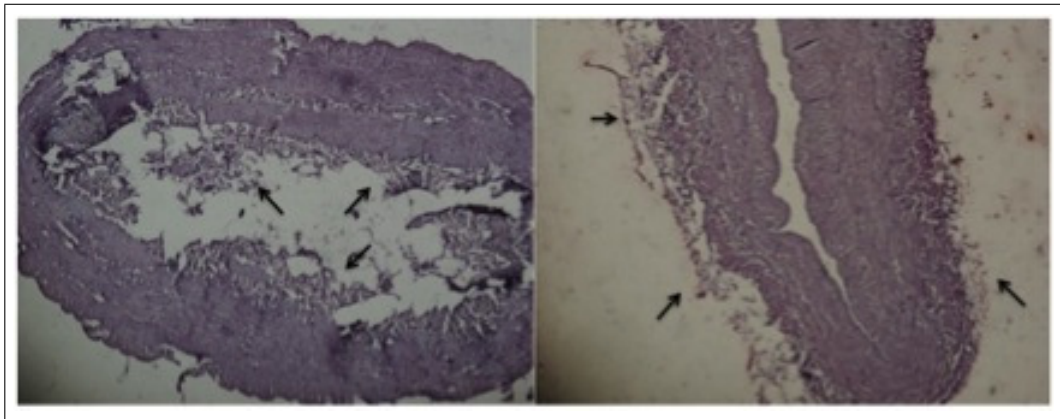


Figure 4.26 Mechanical damages on veins before the laser application. A: Mechanical damage at Tunica Intima, B: Mechanical damage at outside of Tunica Adventitia.

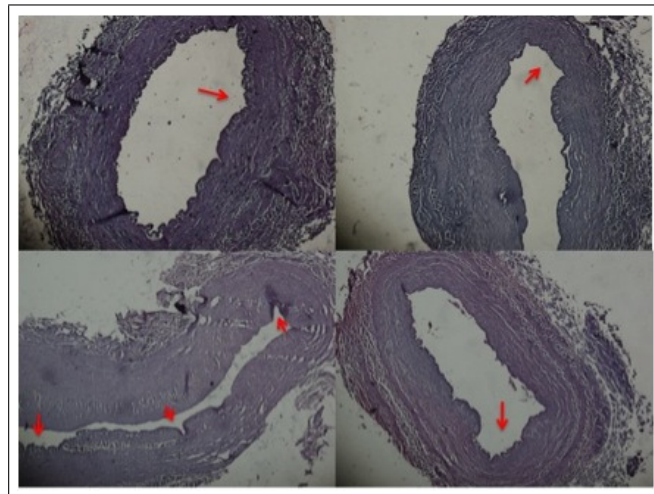


Figure 4.27 Histologic images of cross-sectional vein segments which were irradiated by 1940-nm fiber laser with bare and radial fiber.

It is observed that thermal damage severity increases with the use of 980-nm diode laser. The damages of the 980-nm occur on Tunica Media or between the Tunica Media and Tunica Intima with radial fiber. However, the change of the fiber from radial to bare fiber increases the severity of the damages distinctively. Bare fiber leads to damages on Tunica Adventitia and with u-shaped or v-shaped damages (Figure 4.28).

The severity of carbonization and thermal damage were ranked between 1-4 for all images. The table illustrates the severity range and meaning of the rank points (Table 4.1).

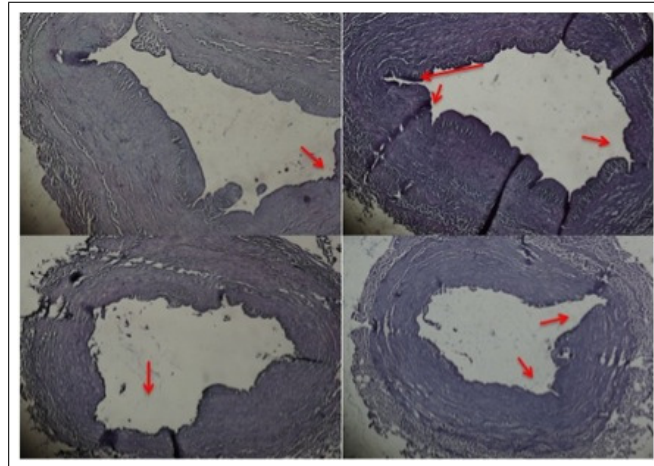


Figure 4.28 Histologic images of cross-sectional vein segments which were irradiated by 980-nm diode laser with bare and radial fiber.

Table 4.1
The meaning of rank points.

Points	Damage Severity
1	Indistinct damage at Tunica Intima
2	Distinct damage at Tunica Intima
3	Distinct damage pass through the Tunica Intima and get the Tunica Media
4	Distinct damage at Tunica Adventitia

It is observed that radial fiber barely decreases the carbonization thermal damage. Applications with bare fiber have significantly more thermal damage for 1940-nm 2W ($0.01 < p \leq 0.05$), 980-nm 8W ($0.001 < p \leq 0.01$) and 980-nm 10W ($0.001 < p \leq 0.01$) than applications with radial fiber. The severity of the carbonization and thermal damage with 1940-nm fiber laser with radial and bare fiber applications are very close to each other (Figure 4.29). x

When 1940-nm fiber and 980-nm diode laser is compared, in the case of radial fiber, 1940-nm fiber laser leads to less thermal damage than 980-nm diode laser. 1940-nm 2W laser application leads to distinctly less thermal damage than 980-nm 8W and 980-nm 10W ($p \leq 0.001$, student t-test). In addition to this, 1940-nm fiber laser at 3W causes significantly less thermal damage than 980-nm diode laser at 10W ($0.01 < p \leq$

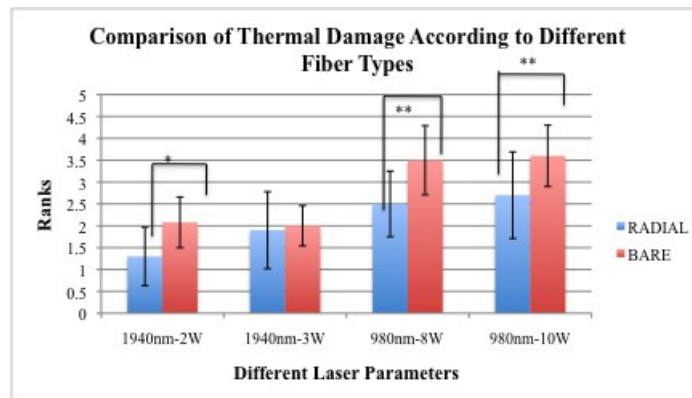


Figure 4.29 The comparison of thermal damage according to different fibers. *, ** are statistically significant results (*, $0.01 < p \leq 0.05$; **, $0.001 < p \leq 0.01$, student t-test).

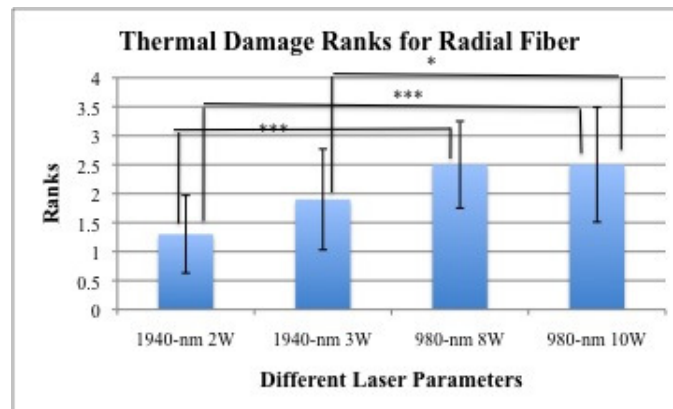


Figure 4.30 The comparison of thermal damage according to different wavelengths with radial fiber. *, *** are statistically significant results (*, $0.01 < p \leq 0.05$; ***, $p \leq 0.001$, student t-test).

0.05). There is no significant difference among other laser application groups (Figure 4.30).

In the case of bare fiber application, the comparison of 1940-nm fiber and 980-nm diode laser illustrated that, 1940-nm fiber laser leads to less thermal damage than 980-nm diode laser. 1940-nm 2W laser application leads to distinctly less thermal damage than 980-nm 8W and 980-nm 10W ($p \leq 0.001$, student t-test). Moreover, 1940-nm fiber laser at 3W causes significantly less thermal damage than 980-nm diode laser at 10W ($0.01 < p \leq 0.05$). There is no significant difference among other laser application groups (Figure 4.31).

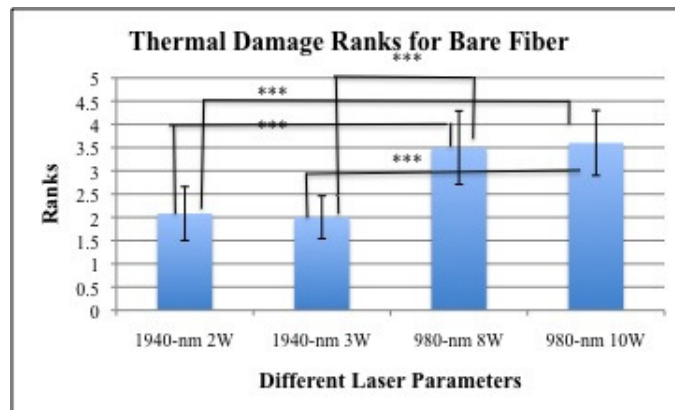


Figure 4.31 The comparison of thermal damage according to different wavelengths with bare fiber. *** is statistically significant results (***, $p \leq 0.001$, student t-test).

5. DISCUSSION

Since EVLA reduces the side effects of classical surgical treatment and is more successful than the other treatment techniques, it has become popular in the treatment of venous insufficiency. EVLA provides shorter operation time, sterile conditions, less recurrence ratios and eliminates the adverse effect of the classical surgery. However, the best treatment parameters are still under investigation to find optimum energy delivery, wavelength and energy delivery techniques. In this study, 980-nm diode laser at 8W and 10W power, which is used prevalently in clinical application and absorbed by hemoglobin highly, and 1940-nm fiber laser at 2W and 3W power, which has high water absorption coefficient are used and compared. Moreover, radial and bare fiber laser is compared for light delivery technique and energy delivery is analysed for all laser application groups.

According to constant power, both in the case of 980-nm diode laser and 1940-nm fiber laser, radial fiber has significantly more inner diameter shrinkage ratio than bare fiber. Radial fiber has homogenous circumferential (360°) laser light delivery; therefore the irradiation area of vessel increases with radial fiber. However, the light delivery of bare fiber is inhomogeneous circumferential to the vessel wall, so nonuniform tissue change is observed with bare fiber which leads to less decrease in inner diameter than radial fiber. In literature, it is proposed that the new technology circularly irradiating laser light fiber confirm the effective occlusion of incompetent truncal veins without thermal damage [8].

When the fiber type is constant, it is analysed that 8W power is more successful than 10W power during 980-nm diode laser application with radial fiber. The energy delivered from 980-nm diode laser at 10W induces more local convection of heat energy than 980-nm diode laser at 8W; therefore, more energy leads to more carbonization instead of shrinkage. In clinical application 980-nm laser application generally is performed between 8W-15W. Comparing the power of lasers, in the study of Kaspar, it

is mentioned that the extent of thermal tissue effects measured by vein shrinkage does not increase when using higher laser power [43].

At constant laser type, it is observed that 1940-nm fiber laser at 2W power leads to more decrease in inner diameter than at 3W power with bare fiber. In the vessel, laser irradiation area increases and fluence ratio decreases with the radial fiber when it is compared with bare fiber [35]. Therefore, at low power ranges high fluence ratio becomes more effective than low fluence ratio which leads to high closure ratio with 1940-nm fiber laser at 2W power with bare fiber.

980-nm diode laser application groups have similar effect on decrease in outer diameter in both of the cases; constant power-different fiber types and different power-same fiber type. In medical applications, 980-nm diode laser at 8W and 10W are used generally. It is suggested that the greatest shrinkage and minimum number of perforations was achieved using lower or medium power between 8 -12 W [43].

1940-nm laser application at 2W with bare fiber results in higher closure ratio than with radial fiber. According to same fiber type and different power, 1940-nm fiber laser at 2W power results more decrease in outer diameter than at 3W power with bare fiber which is a similar result with decrease in inner diameter with 1940-nm fiber laser application. These results support that high fluence ratio with bare fiber become more effective at low power.

Laser energy was delivered continuously and the laser fiber was pulled back manually according to observation of shrinkage. The time of the application was recorded. At 980-nm, Figure 4.3 illustrates that bare fiber duration is significantly shorter than radial fiber duration regardless of power. Since radial fiber decreases the fluence ratio of energy, the shrinkage becomes quicker with bare fiber. Decrease in power decreases the duration of laser application at 980-nm diode laser with radial fiber. Since 980-nm has low water absorption coefficient, delivered laser energy results in intense carbonization. Therefore, at this wavelength increasing delivered laser energy to the vessel wall with high power leads to more carbonization and less shrinkage ratio because of low

absorption coefficient by vessel lumen.

In the case of 1940-nm, there is no significant duration difference between radial and bare fiber at constant power. At low power ranges, laser application duration increases because delivered energy to the vessel lumen decreases; therefore differences in fiber types do not affect the duration distinctly.

In order to analyse the used energy during the laser application, delivered energy to the vessel segment per centimeter (J/cm) is calculated for the laser application groups. In the case of 980-nm diode laser, it is analysed that regardless of power change, laser applications with bare fiber use less energy than with radial fiber during the application. Moreover, with radial power 980-nm laser application at 8W power needs less energy than 10W power. In the case of 1940-nm fiber laser, there is no significant difference among different laser parameter groups. Operation duration is an important criteria for energy; therefore, operation duration and delivered energy per centimeter results are close to each other.

Energy that is needed for the laser application procedure is an important criteria for the clinical operations; therefore, the amount of delivered energy for 1mm shrinkage of inner and outer diameter was calculates. It is observed that 980-nm diode laser needs less energy with bare fiber than radial fiber in terms of 1 mm shrinkage in both inner and outer diameter. At 980-nm diode laser, bare fiber applications are significantly shorter than the radial fiber applications, so that these applications need less energy. Moreover, it is analyzed that at 8W power energy delivered for 1 mm shrinkage is less than at 10W power during 980-nm laser application. Since 8W power leads to more closure of inner and outer diameter in a short time, decrease in inner and oueter diameter in terms of energy is significantly higher than 10W power at 980-nm diode laser. 1940-nm laser application groups have similar results in terms of the amount of energy delivered for 1 mm decrease in inner and outer diameter. Although there are groups which have significantly different results for decrease in inner or outer diameter, the duration of the applications are very close to each other. Therefore, this crieteria for 1940-nm application is affected the closure amount of inner and outer diameter.

Although shrinkage ratio of the 1940-nm is comparable with 980-nm laser applications and duration of the 1940-nm applications is longer than 980-nm with bare fiber, the energy that is delivered during 1940-nm laser applications is significantly less than 980-nm laser applications either with bare fiber or radial fiber. Moreover, the amount of energy delivered for 1 mm decrease in inner and outer diameter with 1940-nm is distinctly less than 980-nm laser applications. Since longer wavelengths is absorbed mainly by water in the vein lumen, less power is adequate for the application. Therefore, need of the energy for longer wavelengths (>1000) during the application is less than the shorter wavelengths (<1000). Also, Mordon *et al* stated that 1320-nm, with a better absorption by the vessel wall, requires less energy to achieve wall damage [36]. Using less energy results in less carbonization and thermal damage which is supported by the histological results of this study. Also, Vulyksteke *et al*'s research, in which the 980-nm and 1500-nm diode lasers, were evaluated histologically. It is proposed that 1500-nm laser has more homogenous vein wall destruction and with less peri-venous tissue destruction and possibly with less postoperative pain [32].

Radial fiber decreases the thermal damage and carbonization both at 980-nm diode laser applications and 1940-nm fiber laser applications. Moreover, it is observed that bare fiber leads to more severe u-shaped and v-shaped damages at Tunica Adventitia with the use of 980-nm diode laser at 8W and 10W. Since radial fiber increases the application area in the vessel where it emanates the laser energy homogeneously. On the other hand the delivery of the laser light is locally focused to application area; therefore fluence rate of energy increases which leads to more damage on the vessel wall. Sroka *et al* proposed that 360° radial fiber decreases the thermal damage and looks promising to induce secure, reliable and reproducible tissue alteration [9].

Histological results show that 1940-nm fiber laser decreases the thermal damage distinctly when it is compared with 980-nm diode laser. The power of the application is 8 and 10W with 980-nm diode laser application; however with 1940-nm the power of the application is 2W and 3W; therefore, high power leads to more thermal damage on vessel wall during the laser application. The energy delivered from the 980-nm diode laser is less well absorbed by the vein wall cells and induces more local convection of

heat energy. Assisting the results of this study, Vuylsteke *et al* compared the effect of 1500-nm laser which has well absorption coefficient by blood and 980-nm laser and they proposed that 1500-nm laser gives less eccentric venous wall injury with broader ulcerations. Deep ulcerations and the more carbonization at the points of direct laser impact were explained by the wavelength difference between 1500-nm which has high water absorption and 980-nm which has high hemoglobin absorption [32]. Also, Ronald Bush *et al* who compared the histological changes of 940-nm diode laser with 1319-nm diode laser stated that 940-nm diode laser has more damage on histologic and ultrasound findings [44].

6. CONCLUSION

In this study, different lasers; 980-nm diode laser and 1940-nm fiber laser and delivery techniques; radial fiber and bare fiber were compared.

In terms of delivery techniques, it is observed that new technology radial fiber decreases the thermal damage and carbonization effect due to homogenous laser energy delivery. Since laser light emanates radially homogenous to tissue, radial fiber does not lead to perforations and deep ulcers. However, the need of energy during the applications increases with the usage of radial fiber. Bare fiber emanates focused light with high fluence rate; therefore perforations and carbonization rate is distinctly observed at the laser applications with bare fiber. However, bare fiber has successful results at low power with 1940-nm fiber laser.

In terms of laser types, although at 1940-nm fiber laser applications, the closure ratio of vein lumen is comparable with 980-nm diode laser applications, need of the energy during the procedure decreases with 1940-nm fiber laser since this wavelength is well absorbed by the water in the vessel lumen cells. Since the delivered energy is low at 1940-nm laser application, thermal damage does not occur as much as 980-nm diode laser. Moreover, amount of closure rate per constant energy is higher with 1940-nm fiber laser than 980-nm diode laser regardless of delivery technique. As a conclusion, 1940-nm fiber laser and radial fiber are promising method in the management of varicose vein.

REFERENCES

1. “Transport in mammals,” <http://www.s-cool.co.uk/a-level/biology/transport/revise-it/transport-in-mammals>, 2011.
2. “Circulatory system veins,” <http://dorientate.blogspot.com/2011/03/circulatory-system-veins.html>, 2011.
3. Fronck, S. H., *The Fundamentals of Phlebology: Venous Disease for Clinicians*, US: American College, 2nd ed., 2004.
4. Wright, D. T., “Veins symptoms and treatments information,” <http://www.veinsguide.com/>, 2011.
5. Goodman, R., “Minimally invasive varicose vein treatment,” <http://www.goodmanvein.com/rlg-procedures.html>, 2008.
6. Huisman, L. C., R. M. G. Bruins, M. van den Berg, and R. J. Hissink, “Endovenous laser ablation of the small saphenous vein: Prospective analysis of 150 patients, a cohort study,” *Eur J Vasc Endovasc Surg*, Vol. 38, pp. 199–202, 2009.
7. Svoboda, K., and S. Block, “Biological applications of optical forces,” *Ann. Rev. Biophys. Biomol. Struct.*, Vol. 23, pp. 247–85, 1994.
8. Schmedt, C.-G., R. Blagova, N. Karimi-Poor, C. Burgmeier, S. Steckmeier, T. Beck, V. Hecht, R. Meier, M. Sadeghi-Azandaryani, B. Steckmeier, and R. Sroka, “Update of endovenous laser therapy and the latest application studies,” *Medical Laser Application*, Vol. 25, no. 1, pp. 34–43, 2010.
9. Sroka, R., K. Weick, and C.-G. S. Mojtaba Sadeghi Azandaryani, Bernd Steckmeier, “Endovenous laser therapy application studies and latest investigations,” *J. Biophoton.*, Vol. 3, no. 5-6, pp. 269–276, 2010.
10. Park, S. W., J. J. Hwang, I. J. Yun, S. A. Lee, J. S. Kim, S. H. Chang, H. K. Chee, S. J. Hong, I. H. Cha, and H. C. Kim, “Endovenous laser ablation of the incompetent small saphenous vein with a 980-nm diode laser: Our experience with 3 years follow-up,” *Eur J Vasc Endovasc Surg*, Vol. 36, pp. 738–742, 2008.
11. Tamar, N., R. R. van den Bos, M. P. Goldman, M. A. Kockaert, T. M. Proebstle, E. Rabe, N. S. Sadick, R. Weiss, and M. H. A. Neumann, “Minimally invasive techniques in the treatment of saphenous varicose veins,” *J Am Acad Dermatol*, Vol. 60, no. 1, 2008.
12. Lim, C. S., and A. H. Davies, “Pathogenesis of primary varicose veins,” *British Journal of Surgery*, Vol. 96, pp. 1231–1242, 2009.
13. Winterborn, J. R., and C. T. F. Smith, *Varicose veins, VASCULAR SURGERY II*, 2010.
14. Kabnick, L. S., “Outcome of different endovenous laser wavelengths for great saphenous vein ablation,” *J. Vasc. Surg.*, Vol. 43, pp. 88–93, 2006.
15. Bos, R. V. D., M. A. Kockaert, H. A. M. Neumann, and T. Nijsten, “Technical review of endovenous laser therapy for varicose veins,” *Eur. J. Vasc. Endovasc. Surg.*, Vol. 35, pp. 88–95, 2008.

16. Allegra, C., P. Antignani, and A. Carlizza, "Recurrent varicose veins following surgical treatment: Our experience with five years follow-up.," *European Journal of Vascular and Endovascular Surgery*, Vol. 33, pp. 751–756, 2007.
17. Nishibe, T. M., and F. Sata, "Long term results of treatments for varicose veins due to greater saphenous vein insufficiency.," *International Angiology*, Vol. 24, pp. 282–286, 2005.
18. Bos, R. V. D., L. Arends, and M. Kockaert, "Endovenous therapies of lower extremity varicosities are at least as effective as surgical stripping or foam sclerotherapy: Meta-analysis and meta-regression of case series and randomized clinical trials.," *Journal of Vascular Surgery*, Vol. 49, pp. 230–239, 2009.
19. Beale, R. J., and M. J. Gough, "Treatment options for primary varicose veins. a review.," *European Journal of Vascular and Endovascular Surgery*, Vol. 30, pp. 83–95, 2005.
20. Merchant, R., and O. Pichot, "Long term outcomes of endovenous radiofrequency obliteration of saphenous vein reflux as a treatment for superficial venous insufficiency.," *Journal of Vascular Surgery*, Vol. 40, no. 500-5004, 2005.
21. Pannier, F., and E. Rabe, "Endovenous laser therapy and radiofrequency ablation of saphenous varicose veins.," *Journal of Cardiovascular Surgery*, Vol. 47, pp. 3–8, 2006.
22. Hingorani, A., E. Ascher, and N. Markevich, "Deep venous thrombosis after radiofrequency ablation of greater saphenous vein: A word of caution. journal of vascular surgery," Vol. 40, no. 500-504, 2004.
23. Zan, S., L. Contessa, and G. Varetto, "Radiofrequency minimally invasive endovascular treatment of lower limbs and varicose veins: Clinical experience and literature review.," *Minerva Cardioangiologica*, Vol. 55, pp. 443–458, 2007.
24. Bergan, J., L. Pascarella, and L. Mekenas, "Venous disorders: Treatment with sclerosant foam. journal of cardiovascular surgery," Vol. 47, pp. 9–18, 2006.
25. Bartholomew, J. R., T. King, A. Sahgal, and A. T. Vidimos, "Varicose veins: Newer, better treatments available.," *Cleveland Clinic Journal of Medicine*, Vol. 72, pp. 312–328, 2005.
26. Bush, R. G., M. Derrick, and D. Manjoney, "Major neuroogical events following foam sclerotherapy.," *Phlebology*, Vol. 23, pp. 189–192, 2008.
27. Forlee, M. V., M. Grouden, and D. J. Moore, "Stroke after varicose vein foam injection sclerotherapy.," *Journal of Vascular Surgery*, Vol. 44, pp. 225–226, 2006.
28. Belcaro, G., M. R. Cesarone, and A. D. Renzo, "Foam-sclerotherapy, surgery, sclerotherapy, and combined treatment for varicose veins: A 10-year, prospective, randomized, controlled trial (vedico trial).," *Angiology*, Vol. 54, pp. 307–315, 2003.
29. Amzayyb, M., R. R. van den Bos, V. M. Kodach, D. M. de Bruin, T. Nijsten, H. A. M. Neumann, and M. J. C. van Gemert, "Carbonized blood deposited on fibres during 810, 940 and 1,470 nm endovenous laser ablation: thickness and absorption by optical coherence tomography," *Lasers Med Sci*, Vol. 25, pp. 439–447, 2010.
30. Desmytte're, J., C. Grard, G. Stalnikiewicz, B. Wassmer, and S. Mordon, "Endovenous laser ablation (980 nm) of the small saphenous vein in a series of 147 limbs with a 3-year follow-up," *Eur J Vasc Endovasc Surg*, Vol. 39, pp. 99–103, 2009.

31. Zimmet, S. E., "Endovenous laser ablation.," *Phlebology*, Vol. 6, pp. 14–51, 2007.
32. Vuylsteke, M., J. V. Dorpe, J. Roelens, T. D. Bo, and S. Mordon, "Endovenous laser treatment: a morphological study in an animal model," *Phlebology*, Vol. 24, pp. 166–175, 2009.
33. Proebstle, T. M., H. A. Lehr, and A. Kargl, "Endovenous treatment of the greater saphenous vein with a 940-nm diode laser: thrombotic occlusion after endoluminal thermal damage by laser-generated steam bubbles.," *J Vasc Surg*, Vol. 35, pp. 729–736, 2002.
34. Fan, C. M., and R. Rox-Anderson, "Endovenous laser ablation: mechanism of action," *Phlebology*, Vol. 23, pp. 206–213, 2008.
35. Zimmet, S. E., and R. J. Min, "Temperature changes in perivenous tissue during endovenous laser treatment in a swine model.," *J Vasc Interv Radiol*, Vol. 14, no. 911-915, 2003.
36. Mordon, S. R., B. Wassmer, and J. Zemmouri, "Mathematical modeling of 980-nm and 1320-nm endovenous laser treatment," *Lasers in Surgery and Medicine*, Vol. 39, pp. 256–265, 2007.
37. Pannier, F., E. Rabe, and U. Maurins, "First results with a new 1470-nm diode laser for endovenous ablation of incompetent saphenous veins," *Phlebology*, Vol. 24, pp. 26–30, 2009.
38. Doganci, S., and U. Demirkilic, "Comparison of 980 nm laser and bare-tip fibre with 1470 nm laser and radial fibre in the treatment of great saphenous vein varicosities: A prospective randomised clinical trial," *Eur J Vasc Endovasc Surg*, Vol. 40, pp. 254–259, 2010.
39. Schmedt, C. G., R. Sroka, S. Steckmeier, O. A. Meissner, G. Babaryka, K. Hunger, V. Ruppert, M. Sadeghi-Azandaryani, and B. M. Steckmeier, "Investigation on radiofrequency and laser (980 nm) effects after endoluminal treatment of saphenous vein insufficiency in an ex-vivo model.," *Eur J Vasc Endovasc Surg.*, Vol. 32, pp. 318–325, 2006.
40. Nwaejike, N., P. D. Srodon, and C. Kyriakides, "5-years of endovenous laser ablation (evla) for the treatment of varicose veins – a prospective study," *International Journal of Surgery*, Vol. xx, pp. 1–3, 2009.
41. Kundu, S., and M. Modabber, "Endovenous ablation for the treatment of varicose veins and lower extremity venous insufficiency," *J Radiol Nurs*, Vol. 30, pp. 36–42, 2011.
42. Puggioni, A., M. Kalra, M. Carmo, G. Mozes, and P. Glosviczki, "Endovenous laser therapy and radiofrequency ablation of the great saphenous vein: Analysis of early efficacy and complications," *J Vasc Surg*, Vol. 42, pp. 488–493, 2005.
43. Kaspar, S., J. Siller, Z. Cervinkova, and T. Danek, "Standardisation of parameters during endovenous laser therapy of truncal varicose veins - experimental ex-vivo study," *Eur J Vasc Endovasc Surg*, Vol. 34, pp. 224–228, 2007.
44. Bush, R. G., H. N. Shamma, and K. Hammond, "Histological changes occurring after endoluminal ablation with two diode lasers (940 and 1319 nm) from acute changes to 4 months," *Lasers in Surgery and Medicine*, Vol. 40, pp. 676–679, 2008.